THE UNIVERSITY OF MICHIGAN

COLLEGE OF ENGINEERING
Department of Nuclear Engineering

Technical Report

IDENTIFICATION OF TRAPPING CENTERS IN CALCIUM TUNGSTATE

Helmut A. Koehler
Chihiro Kikuchi

ORA Project 04381

Supported by:

NATIONAL AERONAUTICS AND SPACE ADMINISTRATION
GRANT NO. NsG 115-16
WASHINGTON, D.C.

administered through:

OFFICE OF RESEARCH ADMINISTRATION ANN ARBOR

July 1968

This report was also a dissertation submitted by the first author in partial fulfillment of the requirements for the degree of Doctor of Philosophy in The University of Michigan, 1968.

TABLE OF CONTENTS

LIST OF TABLES

LIST OF FIGURES

LIST OF FIGURES
(Continued)

LIST OF FIGURES
(Continued)

I SUMMARY OF RESULTS AND HISTORIAL BACKGROUND

The study of trapping centers in crystals and their effect on the physical properties of the solid has been a major area of interest in Solid State Physics. A large variety of physical measurements and theoretical calculations have been performed for many years to identify these centers and for the subsequent control of their occurrence. Inspite of this large effort, no present information is available about the identity of trapping centers in $CaWO_4$ crystals.

The purpose of this thesis then is to report the first identification of three trapping centers in nominally pure calcium tungstate ($CaWO_4$). The importance of this work lies in the method illustrated for identifying trapping centers. This identification was made by correlating thermoluminescence (TL) and electron spin resonance (ESR) measurements*.

The TL measurements of nominally pure $CaWO_4$, after gamma-irradiation at 78°K, provided information about the trap energies of the trapping centers. Three major TL peaks of pure $CaWO_4$ were observed at 155°K, 225°K, and 290°K. The trap energies corresponding to these TL peaks are 0.36 ev, 0.55 ev, and 0.72 ev respectively. These values are calculated by a method combining Randall-Wilkins' and Vasileff's theories. Both theories apply to the thermal ionization of electrons from trapping centers. This method is compared to other commonly used procedures for finding trap energies from TL curves.

---

*Hereafter, TL will refer to thermoluminescence and ESR to electron spin resonance.

Information about the lattice sites of the electrons in the trapping centers was provided by ESR measurements of gamma-irradiated nominally* pure $CaWO_4$. The ESR spectra of pure $CaWO_4$ at 78°K indicated that three paramagnetic centers are formed by gamma-irradiation. These centers are identified with paramagnetic tungsten (W^{+5}) and niobium (Nb^{+4}) ions in the tungsten sites. Partial annealing of the samples removed the first paramagnetic tungsten $(W^{+5})_A$ spectrum**. The g-value was 2.009 with the magnetic field in the (001) direction. A similar heating cycle removed the first TL peak. This provided sufficient evidence for associating the trapping centers responsible for the first TL peak with tungsten $(W^{+5})_A$ ions. Similar differential thermal annealing of the samples removed the second paramagnetic tungsten $(W^{+5})_B$ spectrum (g_{001}=1.843) and the niobium (Nb^{+4}) spectrum (g_{001}=2.021). The disappearance of these two spectra was associated with the removal of the second and fourth TL peak respectively. This provided convincing evidence for identifying the trapping centers responsible for the second and fourth TL peak with tungsten $(W^{+5})_B$ ions and niobium (Nb^{+4}) ions respectively.

In view of these experimental TL and ESR results, the fourth TL peak is attributed to impurity ions whereas the first and second TL peak are related to lattice defects. The assignment of the Nb^{+4} ion identified with the fourth TL peak to a tungsten site and a NbO_4^{-4} complex, followed from a comparison with a similar spectrum observed by Chu[67] for paramagnetic niobium in gamma-irradiated $CaWO_4$. The tungsten $(W^{+5})_A$ ion

---

* The expressions "nominally pure $CaWO_4$" and "pure $CaWO_4$" refer to $CaWO_4$ as grown with no intended impurities

** Subscript A distinguishes the first tungsten spectrum from the second tungsten spectrum B

identified with the first TL peak, is assigned to a WO_4^{-3} complex with a nearby WO_3 and NbO_4^{-3} complex on the basis of the directions and values of the principal axes of the g-tensor, the electron transfer from $(W^{+5})_A$ to Nb^{+5} ions, and the absence of the $(W^{+5})_A$ spectrum in all rare earth ion doped $CaWO_4$ crystals. Furthermore, it is shown that the presence of WO_3 in $CaWO_4$ and the substitution of WO_3 for WO_4^{-2} is highly probable. The tungsten $(W^{+5})_B$ ion identified with the second TL peak, is tentatively assigned to a WO_3^{-1} complex with a nearby calcium deficiency. This conclusion was reached by considering the directions and values of the principal axes of the g-tensor and the occurrence of the strong $(W^{+5})_B$ spectrum in all rare earth ion doped $CaWO_4$ samples.

Calcium tungstate has been the subject of investigations for the past twenty years. Oszy[1] and Kröger[2] investigated nearly two decades ago the spectral and temperature dependence of the absorption-, emission-, and excitation spectra of $CaWO_4$ in powder and crystalline form. Gillette[3], Beard, Kelly and Mallory[4], and Sayer and Hardy[5] studied the application of $CaWO_4$ crystals as gamma scintillation counters. Their measurements of the temperature dependence of the scintillation efficiency and of the luminescence decay time indicated that the values of the decay time depend in part on the crystals used. Sayer and Hardy attributed this variation in decay time to the differences in the density of impurities or trapping sites. Because of the relatively long scintillation decay time (5 to 30 microseconds) no further interest was shown in $CaWO_4$ single crystals until the discovery of laser action from rare-earth ions in $CaWO_4$. This renewed interest led to a systematic investigation of the rare-earth ions[6-14] and the properties of these ions in $CaWO_4$[15-24]. New efforts for improving the quality of $CaWO_4$ single crystals stimulated further research of the calcium tungstate material[25-35], such as the investigation of impuri-

ties and trapping sites.

Attempts have been made for the past decade to study the trapping sites in $CaWO_4$ by thermoluminescence (TL)[5,36-42]. Table I shows a summary of some of those results. It is indicated that the corresponding TL peak temperatures are in reasonable agreement and independent of the mode of excitation. The usefulness of the TL measurements lies in the information it furnishes concerning the impurity energy levels in the band gap. Several methods[43-56] are available for calculating these energy levels or trap energies from the experimental TL curves. Randall and Wilkins[46], and Vasileff[56] describe two of those methods. Sayer and Souder[40] used a modification of Randall's and Wilkins' method for finding the trap energy values of the three major TL peaks of pure $CaWO_4$.

General disagreement exists in the interpretation of the thermoluminescence (TL) and thermally stimulated current (TSC) measurements. For instance, Cook[36] reported a close correspondence between the TL- and TSC curves which suggested the emptying of the traps through the conduction band. However, Sayer and Souder[40] observed no such correlation between the TL and TSC curves. They suggested the trapping of electrons and holes at impurity centers external to the luminescence centers (WO_4^{-2}). Levshin, Guman and Karzhavina[37], Hahn and Lertes[38], and Sayer and Hardy[5] reported a dependence of the luminescence decay curves on the form of excitation (alpha-, electron-, and gamma irradiation). Reference 37 and 38 proposed that this dependence is caused by new trapping sites which are created in the luminescence centers (WO_4^{-2}) by radiation. It is apparent from these suggestions of possible defect sites that no definite identification of trapping centers has been possible from TL measurements alone.

TABLE I

SUMMARY OF PREVIOUS RESULTS FROM THERMOLUMINESCENCE OF $CaWO_4$

Author	Mode of Excitation	Approx. Peak Temp. (°K) and Trap Energies (ev)	Comments
Cook[36] (1958)	gammas at 100° K	178°K 226°K 313°K	Traps empty through conduction band
Levshin[37] Guman (1959) Karzhavina	electrons at 88° K	153°K 240°K	Crystal defects produced by electrons
Hahn[38] (1962) Lertes	electrons at 88° K	155°K 270°K	Traps do not empty through conduction band. Traps created by electrons in luminescence centers (WO_4^{-2})
Sayer[5] (1965) Hardy	alphas at 100° K	150°K 205°K 295°K	TL depends on crystals used and mode of excitation (α, β, γ)
Bräunlich[39] Reibner (1965) Scharmann	electrons at 90° K	160°K 226°K 263°K	Traps do not empty through conduction band. Traps in luminescence centers (WO_4^{-2})
Sayer[40] (1967) Souder	gammas at 85° K	160°K (0.32 ev) 219°K (0.44 ev) 305°K (0.62 ev)	Traps empty through conduction band. Traps originate at impurity centers external to luminescence centers (WO_4^{-2}). Strong influence of impurities on TL curves

Two ESR spectra of paramagnetic tungsten similar to those of $(W^{+5})_A$ and $(W^{+5})_B$ observed in this investigation, were reported by Zeldes and Livingston[60] in gamma-irradiated $CaWO_4$. These two spectra were attributed to two tungsten atoms with a hole and to one tungsten atom with an electron, since the spectra were formed at an equal rate and disappeared simultaneously upon warming to approximately 141°K. This interpretation of the trapping centers is not supported by the results presented in the following chapters.

II THERMOLUMINESCENCE INTENSITY

This chapter describes the three major TL peaks obtained from TL measurements on single crystals of pure $CaWO_4$. The method used for the determination of the trap depth and the frequency factor of the three trapping centers responsible for the three TL peaks is discussed and compared with other commonly used methods.

2.1 Introduction

This section gives a brief description of the origin of TL. The basis of the discussion is an insulating crystal whose energy levels are shown schematically in Figure 1.

The valence band A represents the highest energy states of bound electrons in the crystalline solid. The lowest energy states of the free electrons correspond to the conduction band B. Impurity atoms or lattice irregularities give rise to localized electron states C, D and F, which may occur between the energy bands of the pure crystal. Electrons can be excited into the conduction band from A or C by radiation, such as gamma-rays. The passage of gamma-rays through a solid may cause extensive ionization and electron excitation, since the interaction of gamma-rays with matter occurs principally by the photo-electric effect, the Compton effect, and pair production. Although gamma-rays can produce displaced atoms in solids, this mechanism is usually neglected since the efficiency of such a process is quite low.

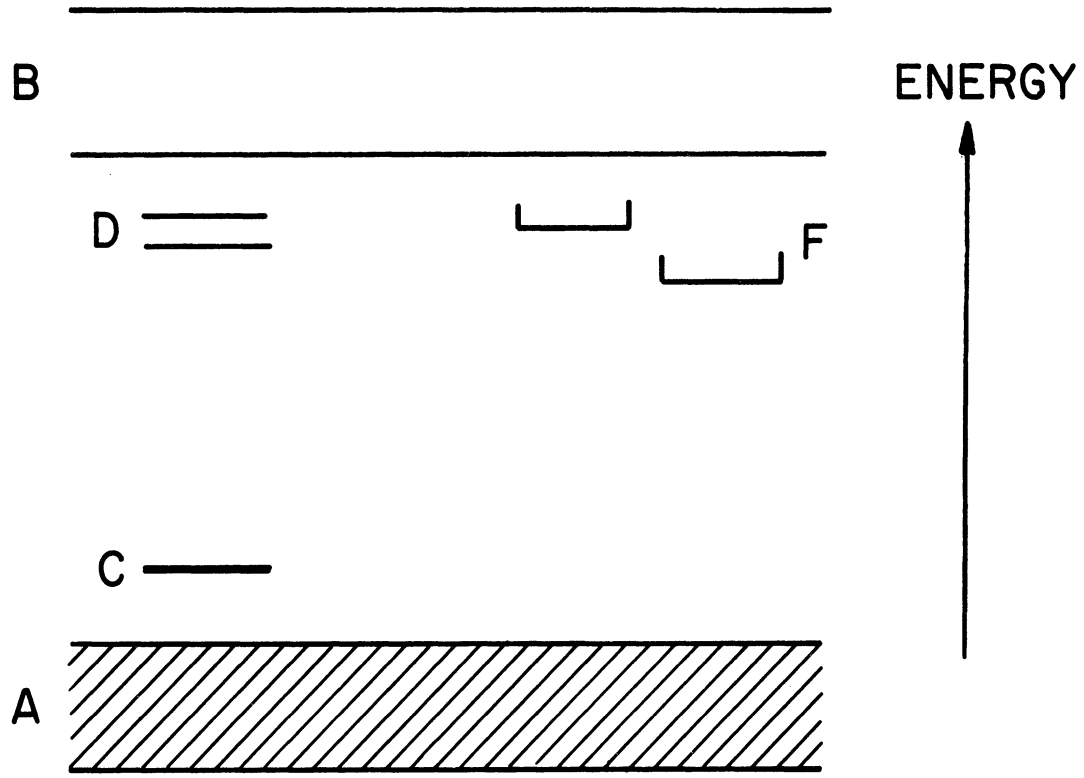

Figure 1

Band Model of Insulator

Electrons in the levels F near the conduction band may be excited by thermal or optical radiation into the conduction band. These excited electrons then return to the ground state at luminescence centers; the electron makes a transition first from B to D and then from D to C. The second transition is commonly associated with the emission of light. This emission is referred to as thermoluminescence, if the electrons are released from the levels F by thermal agitation. The levels F are normally empty since they are only a small way below the conduction band. They may therefore capture electrons excited into the conduction band. These levels are called electron traps because of their relatively high electron capture probability at low temperature.

An electron trap can be compared with a potential well. The frequency of the periodic motion of the electron in the potential well is commonly referred to as the frequency factor. For the electron to remain in the potential well, the value of this frequency factor must be less than the lattice frequency since the lattice vibrations are responsible for the energy transfer between the trapped electron and the lattice. Depending upon the depth of the potential well, a temperature is reached during heating at which the energy of the trapped electron exceeds the depth of the well and the electron becomes ionized. The amount of thermal energy which raises the electron into the conduction band is called the trap depth or trap energy. The TL curve is a recording of the luminescence intensity resulting from the recombination process of these ionized electrons as a function of temperature. The intensity of the TL increases and decreases in accordance with the electron trap densities. With increasing temperature, the electrons escape first from those traps which are nearest the conduction band. Upon further heating, deeper

lying traps begin to empty causing again a variation in the emission intensity. Thus, the final TL curve consists of several distinct TL peaks, if the electron traps are well separated in energy.

2.2 Experimental Procedure and Apparatus

Thermoluminescence measurements were performed on single crystals of nominally pure $CaWO_4$ obtained from Isomet Corporation and Harry Diamond Laboratories. These crystals were grown by the Czochralski method[25] from pure $CaWO_4$ powder supplied by the Sylvania Electric Products Division. The impurity concentration of this powder was given by the Sylvania Spectroscopic Laboratory as less than 0.01% of Al, Ba, Cr, Fe, Mg, Mn, Mo, Pb, Si, and Ti. No mention was made of V, Nb, and Ta. The crystals, as grown, varied in diameter from 5 mm to 10 mm while the length varied between 1 cm and 3 cm. These crystals were cut into 1 mm to 2 mm sections and mechanically polished with Al_2O_3 powder. Typical dimensions of the samples used in the TL experiments were approximately 4x4x2 mm^3.

These crystal sections were gamma-irradiated at 78°K, receiving a total dose of approximately 300 kilorads or $10^{15\pm1}$ gammas. All crystals appeared dark after gamma-irradiation. The samples were then transferred in liquid nitrogen to a copper sample holder mounted at the bottom of the cold finger. The cold finger was inserted into a cryostat which was evacuated to a pressure of approximately 4×10^{-3} mm of Hg. A negligible amount of frost formed on the samples during this transfer of the cold finger to the cryostat.

Thermoluminescence was obtained by heating the gamma-irradiated crystals from 78°K to 350°K. This heating was achieved by using a nichrome heater, placed in a quartz tube surrounded by a copper sleeve. This

assembly was inserted into the cold finger. The heating rates of the crystals were varied from one experiment to the other by changing the voltage to the heater with a Cenco Variac. Approximately eight TL curves were obtained for different rates between 2°K/min and 17°K/min. Relatively low heating rates were used to reduce the thermal capacity effects in the samples. The temperature of the crystals was monitored with a copper-constantan thermocouple and recorded with a synchronous speed recorder. This provided a trace of temperature versus time.

The luminescence emitted by the sample was chopped mechanically at a rate of 90 cycles per second. The light was focused onto the entrance slit of a monochrometer set at 4900Å corresponding to the maximum TL intensity of pure $CaWO_4$. The diffracted light was detected by a photomultiplier placed at the exit slit of the monochrometer. The output of the photomultiplier proportional to the emission intensity was amplified and applied to a second synchronous speed recorder. This recorder provided a trace of intensity versus time. The speed of this recorder was synchronized with the recorder monitoring the temperature. Combining the traces from both recorders resulted in the standard TL curves of intensity versus temperature.

The heating of the crystals was stopped at approximately 350°K. The samples were then annealed at 700°K for 40 hours.

The sample holder on which the crystals were mounted is shown in Figure 2. This holder was basically the same as the one used by Barnes[61] It consists of a flat, vertical copper back-plate, with a hole in the center for transmission measurements, and a copper clamp for holding the sample firmly in place. Two cooling channels provided a nearly uniform cooling of the sample holder. Also shown in Figure 2 is the point at which the

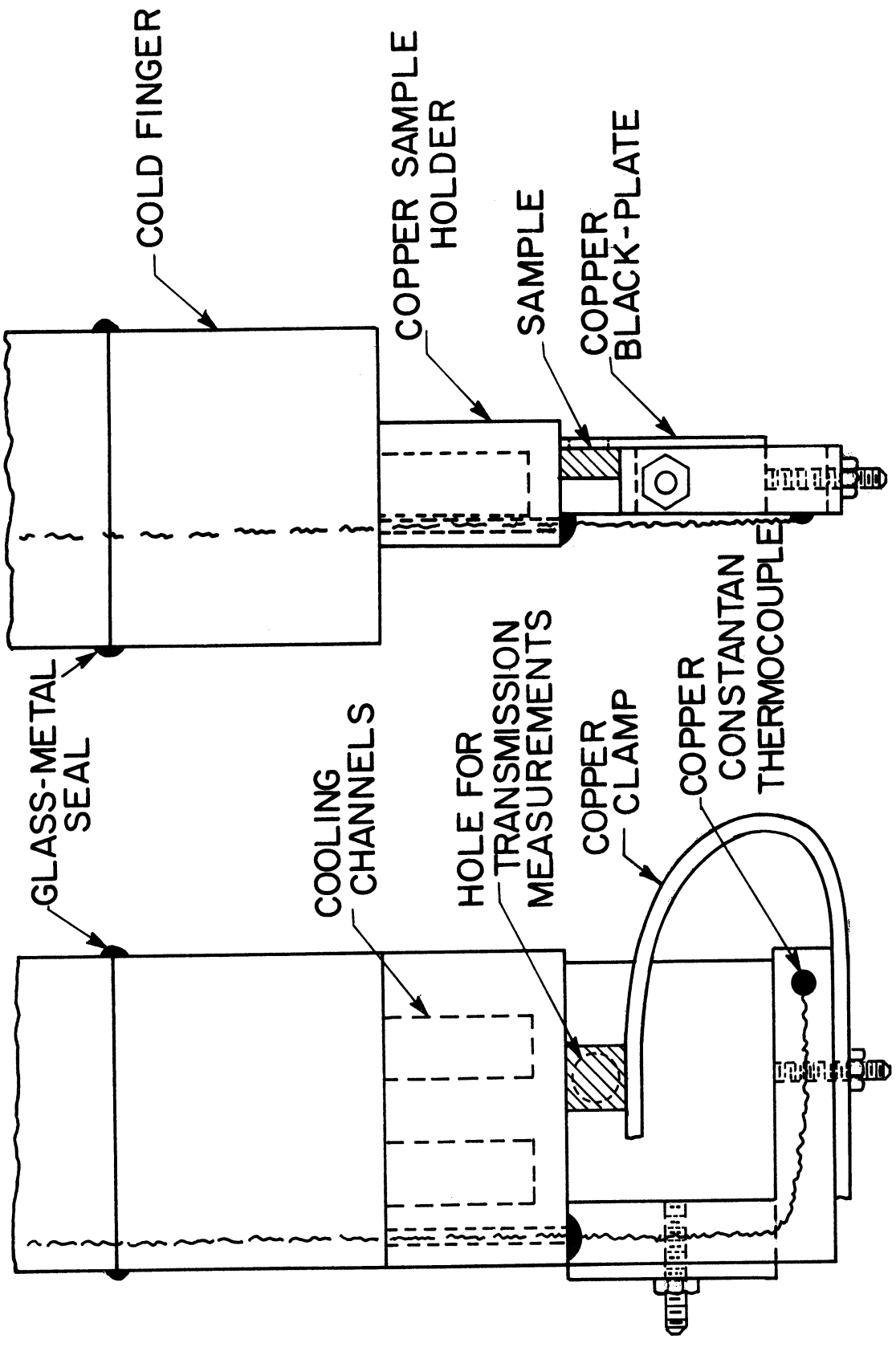

Figure 2

Sample Holder for Optical Measurements

temperature of the crystal was measured.

A schematic diagram and a pictorial view of the experimental apparatus used for the TL measurements of gamma-irradiated $CaWO_4$, are shown in Figures 3 and 4 respectively. The cryostat (6) which contained the sample is equipped with three quartz windows, one inch in diameter and 90 degrees apart. The distance from the sample to the inside of the windows is approximately one inch. This cryostat is firmly held in place in front of the entrance slit of a Bausch and Lomb grating monochrometer (1) of 500 mm focal length. The monochrometer grating is blazed for 7500 Å with 600 grooves per millimeter and an efficiency of 25% at 5000 Å. The reciprocal linear dispersion for this instrument is 33 Å/mm.

An RCA 6199 photomultiplier tube (2), with an S-11 photocathode response is used to cover the spectral range from 4000 Å to 6500 Å. This photodetector is mounted in an Electro-Optics Associates, PM-101 photomultiplier assembly and cooled to 200°K. The DC voltage for the photomultiplier is supplied by a Hammer Electronics Co., Inc., type N-4035, regulated high-voltage power supply.

The signal from the photomultiplier tube (2) is applied directly to the input terminals of a Princeton Applied Research, Model JB-5, lock-in amplifier (3). The maximum overall gain of the amplifier is approximately 10,000. This amplifier is a phase sensitive or synchronous detector and acts like a narrow band pass detection system. The reference or synchronous signal is obtained from a silicon cell, excited by the light of a tungsten lamp. This light is chopped at the same rate of 90 cycles per second as the signal light.

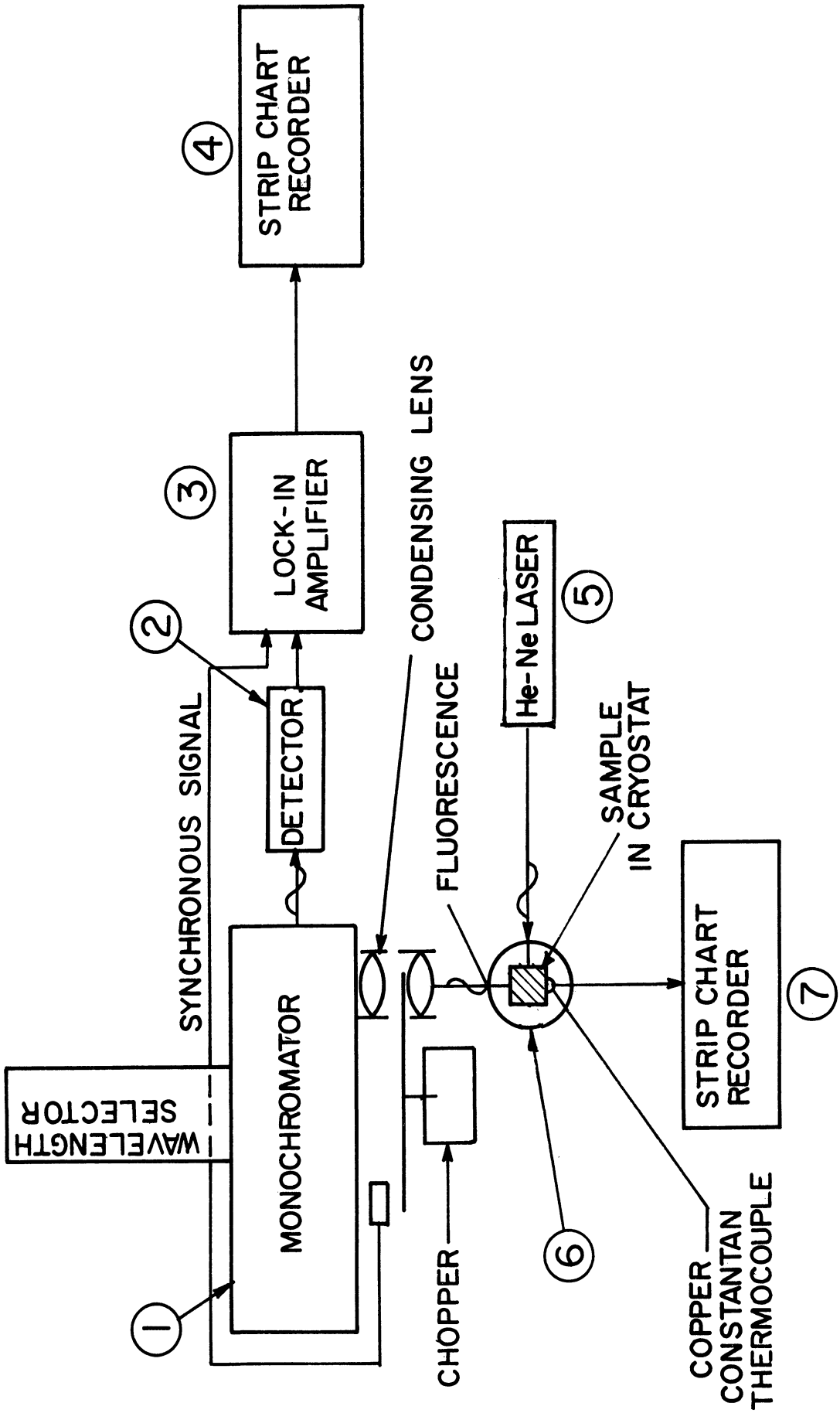

Figure 3

Schematic Diagram of Experimental Apparatus

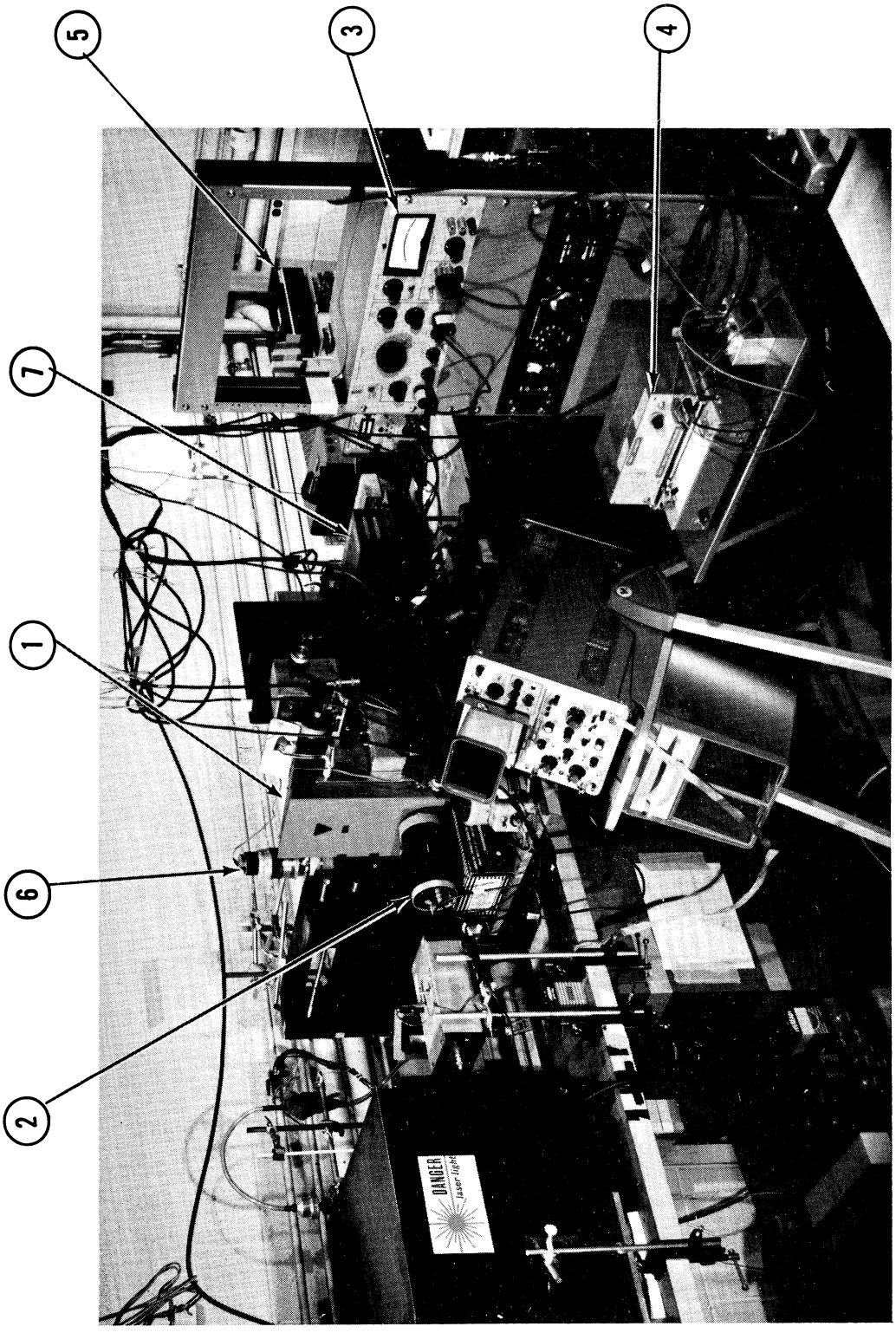

Figure 4

Pictorial View of Experimental Apparatus

The DC output of the amplifier is applied to a Varian Associates, Model G-10, synchronous speed Graphic recorder (4) of 50 millivolt full scale and chart speeds of 2 inch/minute and 6 inch/hour. This recorder provided the trace of the TL intensity versus time.

A similar Varian recorder (7) is used to monitor the temperature of the samples. This resulted in the trace of temperature versus time.

Also shown in Figures 3 and 4 is a helium-neon gas laser (5). The 6328 Å line of the continuous, two milliwatt, Spectra-Physics, Model 130, helium-neon gas laser was used for absolute measurements of the electron trap densities. For these measurements, the number of photons in the laser beam was determined with an Eppley Laboratory Inc., No: 4940, circular type thermopile (4.70 microwatts/microvolt). The Varian recorder (4) was then calibrated in terms of the number of laser photons incident on the entrance slit of the monochrometer (1). The calibration constant (4.5×10^9 photons/sec/recorder chart units) for this recorder was adjusted for the spectral response of the system at 6328Å.

The helium-neon gas laser was also used for proper alignment of all the optical components which were placed on Spindler and Hoyer, triangular optical benches.

The gamma-irradiations were made with a calibrated, 8000 curies, cobalt-60 source in the Phoenix Memorial Laboratory of the University of Michigan. The source was a cylindrical shell of 31 cm length and 9 cm inside diameter. The average flux at the crystal position in the center well was approximately 10^{13} gamma/second or 150 kilorads/hour.

2.3 Experimental Results

The experimental TL results are presented in two parts. The TL

curves of nominally pure $CaWO_4$ are discussed at first. This is followed by the calculation of the trap depth of the trapping centers, corresponding to the TL peaks.

2.3a Thermoluminescence Curves

A typical TL curve of nominally pure $CaWO_4$ after gamma-irradiation of 300 kilorads at 78°K is shown in Figure 5.

Three major TL peaks are indicated at approximately 160°K, 230°K, and 295°K with the corresponding heating rates of 9°K/min, 7.5°K/min, and 5.5°K/min respectively. These three peaks referred to as the first, second, and fourth TL peak, were investigated in detail. The third TL peak was not included in this investigation because of the relatively low peak intensity. Only the average values of the heating rate are indicated since the latter varied slightly during warm-up through the TL peaks. The largest variation in heating rate (2°K/min) was observed for the first TL peak at 160°K whereas the smallest change in heating rate (0.6°K/min) was noted for the fourth TL peak at 295°K.

Additional TL peaks were observed at approximately 108°K, 135°K, 175°K, and 260°K. The TL peaks at 135°K and 175°K occurred on the low and high temperature side of the first TL peak respectively, whereas the peak at 260°K was found on the low temperature side of the third TL peak. These additional TL peaks were not well defined since their intensity was reduced by a factor of 100 relative to the three major TL peak intensities. Therefore, they are not indicated in Figure 5.

The TL curves of the $CaWO_4$ crystals obtained from Isomet Corporation and Harry Diamond Laboratories were normalized at the first TL peak because the position and the size of the samples differed slightly from one experiment to the other and because absolute measurements of the TL

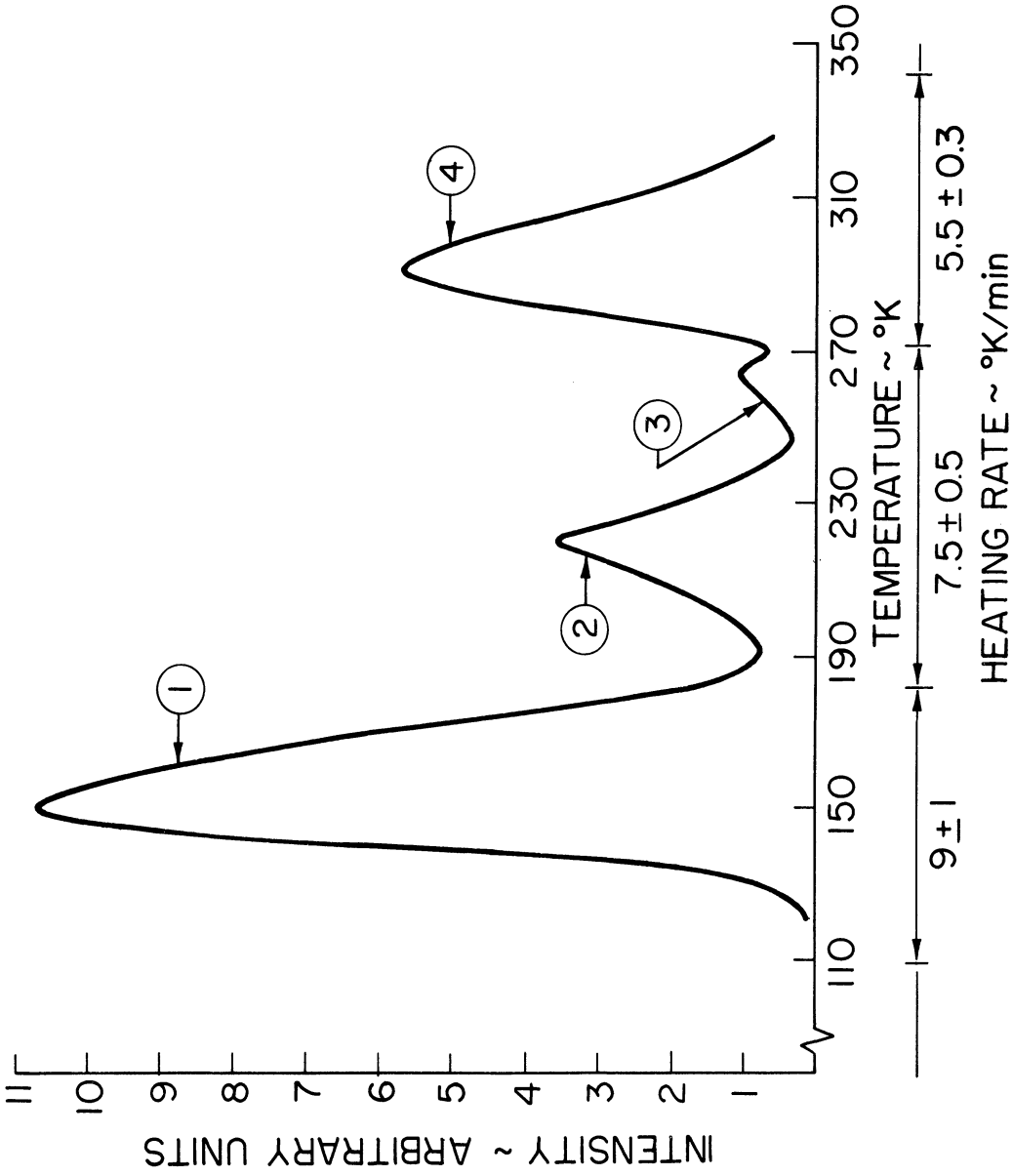

Figure 5

Typical TL Curve of Nominally Pure $CaWO_4$ After Gamma-irradiation of 300 Kilorads at 78°K

peak intensities were not performed. The normalized TL curves showed the same TL peak temperatures for both samples. This was an indication that identical trapping centers are present in both crystals. However, the electron trap densities varied in both crystals. This was evidenced by the different peak intensities of the second and fourth TL peak*. These intensities (arbitrary units) were the following:

Sample	First TL Peak	Second TL Peak	Fourth TL Peak
HDL	11	4	6
ISOMET	11	22	31

The experimental values which were obtained from the TL curves are the peak temperature, the peak intensity, the peak starting temperature, and the heating rate. These quantities are used in the Randall-Wilkins[46] equation for finding a relationship between the trap depth and the frequency factor.

The TL curves of nominally pure $CaWO_4$ obtained for different heating rates, indicate that the TL peak temperature increases with increasing heating rate. Such a dependence of the TL peak temperatures on the heating rates is shown in Figure 6 for the first-, second-, and fourth TL peak of pure $CaWO_4$.

This dependence of peak temperature on heating rate was investigated in the region of 2°K/min to 17°K/min. It is shown that the relationship between peak temperature and heating rate is the same for the three

---

* The TL curves were normalized at the first peak

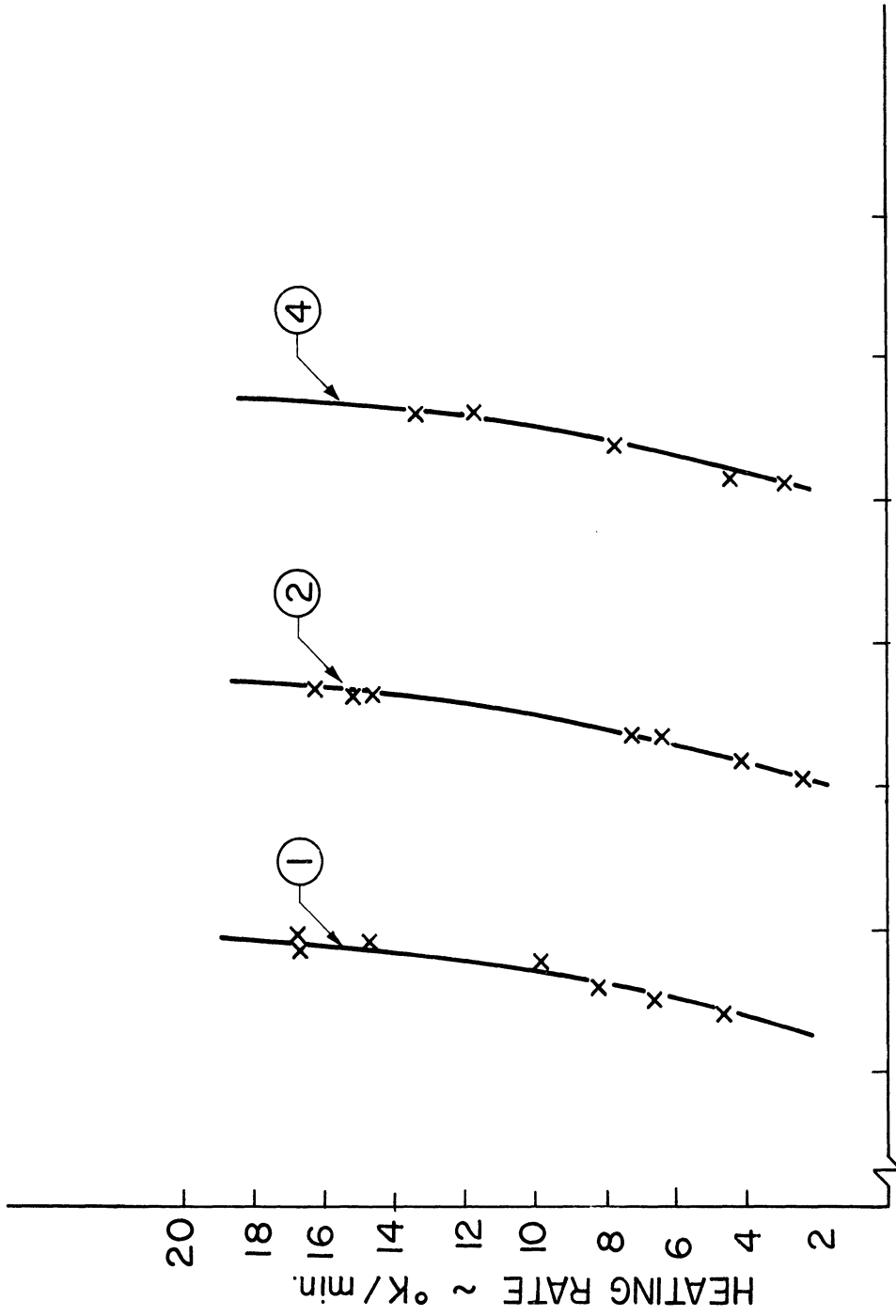

Figure 6

Heating Rate versus Peak Temperature for Major TL Peaks of Pure $CaWO_4$ After Gamma-irradiation of 300 Kilorads at 78°K. Emission Monitored at 4900Å

major TL peaks of pure $CaWO_4$. The increasing peak temperatures with higher heating rates observed for each TL peak, can be explained by the temperature lag between the measured temperature of the cold finger and the true temperature of the sample at elevated heating rates. However, it is not understood why the TL peak temperature should become nearly independent of the heating rate above approximately 20°K/min[38] as seems to be indicated in Figure 6.

It will be shown later that the methods available for finding approximate values for the trap depth and the frequency factor make use of the TL peak temperature and heating rate. For instance, a peak temperature of 160°K and a heating rate of 9°K/min corresponding to the first TL peak of pure $CaWO_4$ shown in Figure 5, were used in Randall-Wilkins' equation to find a relationship between the trap depth and the frequency factor for the first TL peak.

However, a TL peak temperature independent of heating rate must be found for the calculation of the trap depth and the frequency factor which makes use of the peak temperature value but not the heating rate. Such temperature values are obtained by considering the peak intensity and corresponding peak temperature ratios of each TL curve. This procedure eliminated the influence of the heating rate on the TL peak temperature and the effect of the sample position and size on the TL peak intensity. Assuming the first TL peak at 155°K, the resulting constant peak temperature ratios were solved for the temperatures of the second and fourth TL peak. The values are 225°K and 290°K respectively. These temperatures, referred to as "effective TL peak temperatures", were used in Vasileff's expression[56] for finding a relationship between trap depth and frequency factor. This will be discussed in the next section.

2.3b Trap Depth

This section discusses the method used for the determination of the trap depth and the energy and temperature dependent frequency factor of the three major TL peaks of pure $CaWO_4$. The method consists of a combination of Randall-Wilkins'* and Vasileff's expressions. The trap depth and the frequency factor for the first TL peak are determined at first from Randall's expression. Using this value of the trap depth, it is shown that the same frequency factor is obtained from Vasileff's expression. Both expressions are then used to determine a numerical relationship between the trap depth and the frequency factor for the three major TL peaks of $CaWO_4$. This resulted in two curves of trap depth versus frequency factor for each TL peak. The intersection of these curves provided then the values for the trap depth and the frequency factor corresponding to the three significant TL peaks.

Randall's expression was derived in Appendix I and indicated there as equation (6). This equation is shown below:

$$(6) \qquad \frac{I}{n_o} = s \exp\left[E/kT\right] \exp\left[-\frac{s}{\beta}\int_{T_i}^{T} \exp\left(-E/kT'\right) dT'\right]$$

It relates the luminescence intensity (I) emitted upon the thermal release of trapped electrons, to the temperature (T), heating rate (β), trap depth (E), and frequency factor (s). The quantities n_o, T_i, and k are the number of trapped electrons at T=0, the starting temperature, and the Boltzmann's constant respectively. This equation considers only the

---

* Hereafter, the expression derived by Randall and Wilkins will be referred to as Randall's equation

escape of the electrons from the trapping centers. It is based upon the assumption that the trapped electrons have a Maxwellian distribution of thermal energies. To derive equation (6) it was tacitly assumed that the frequency factor s is independent of energy and temperature, although there is no evidence for this. Also implicit in the derivation is the assumption that no temperature dependent, non-radiative de-excitation processes are present in the temperature range of the TL.

Randall's expression describes the curve of intensity versus temperature of a TL peak. This expression evaluated at the maximum TL peak intensity and temperature (T_{max}), is indicated by equation (8) in Appendix I; i.e.:

$$(8) \qquad s = \frac{\beta}{T_{max}} \left(\frac{E}{k T_{max}}\right) \exp\left(\frac{E}{k T_{max}}\right)$$

This equation, which is also referred to as Randall's equation, was used at first to find a relationship between the trap depth E and the frequency factor s from the experimental TL peak temperature T_{max} and the corresponding heating rate β. Figure 7 shows this equation and three calculated sets of values of E and s for the first TL peak of pure $CaWO_4$ at 160°K (Figure 5). These three sets of values are indicated by the triangle , square , and diamond . A straight line of log(s) versus E was drawn through the three calculated points, because the frequency factor is governed by the exponential of peak temperature and trap energy in the range of TL ($E/kT \gg 1$). Nearly the same frequency factor values were obtained for different peak temperatures (160 ± 5°K) and heating rates (9 ± 1°K/min) corresponding to the first TL peak (Figure 6), since the ratio (β/T_{max}^2) only changed by a few percent. That is, the

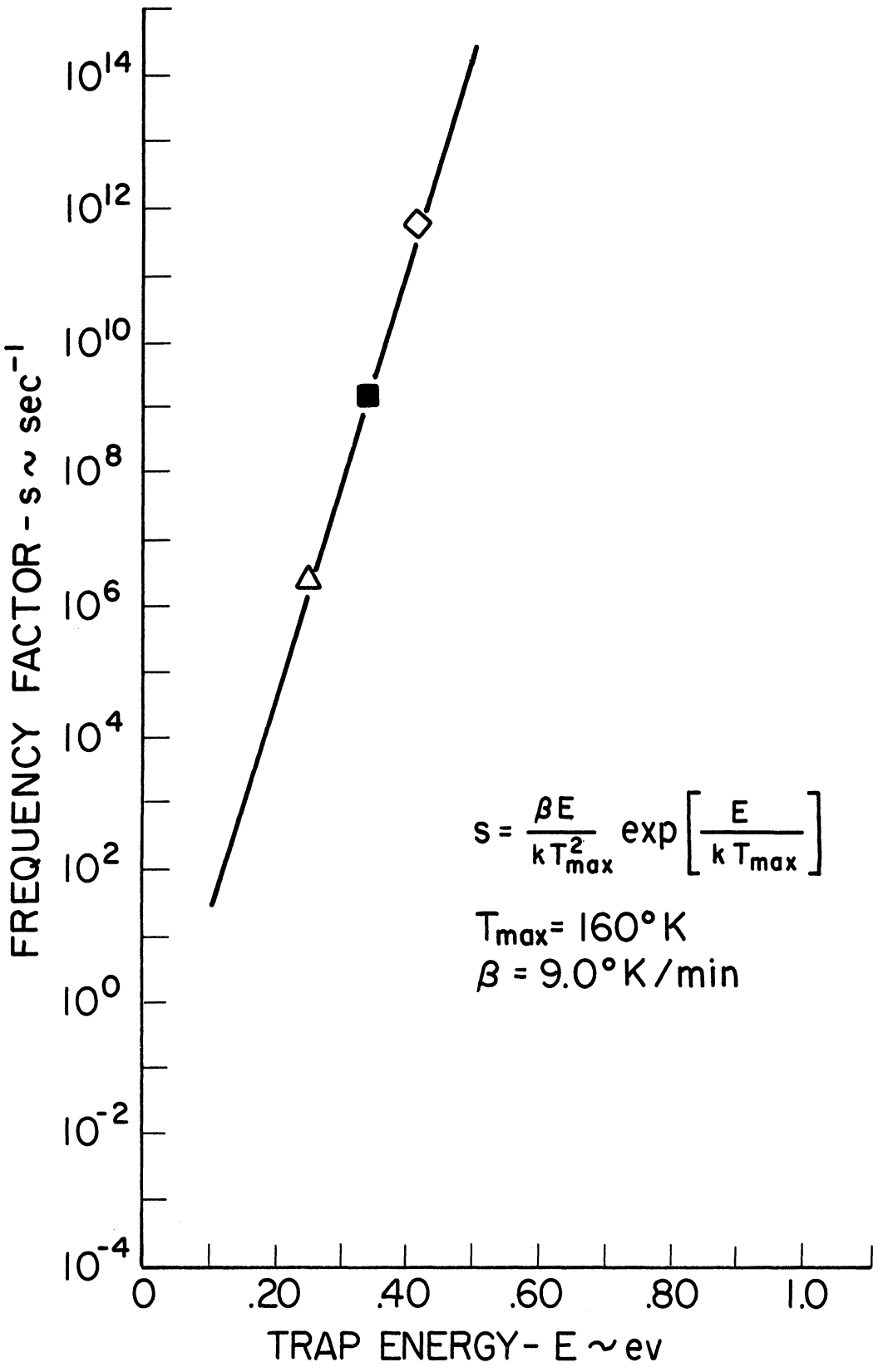

Figure 7

Frequency Factor Versus Trap Energy of First TL Peak of Nominally Pure $CaWO_4$

position and slope of the straight line shown in Figure 7 was considered unchanged in view of the experimental accuracy of determining the TL peak temperature ($\pm 5^{\circ}K$) and corresponding heating rate ($\pm 1^{\circ}K/min$). It is interesting to note that equation (8) does not apply when the heating rate approaches zero. This agrees with the experimental fact that it is physically impossible to observe TL at zero heating rate.

The three sets of values of E and s previously discussed, were then used in Randall's equation (6) together with the peak temperature T_{max}, starting temperature T_i, and heating rate β of the experimental first TL peak of pure $CaWO_4$. Figure 8 shows the three resulting curves of TL intensity (I/n_o) versus temperature T by the same symbols which were previously used to identify the three sets of values for E and s. These curves were normalized to the first TL peak of pure $CaWO_4$ shown by the circles. The numerical values for the trap depth and the frequency factor and Randall's equation are also indicated.

A comparison of the calculated curves shows that decreasing the values of the trap depth and the frequency factor will increase the half-width of the calculated curve. Since most major TL peaks are associated with small intensity peaks, causing an increase in the half-width of the major TL peak, it is not surprising to expect low values for the trap depth E and frequency factor s obtained from the curve fitting method. In fact, reduced values of E and s can be expected from any method which is derived in part from Randall's equation and uses the envelope of the experimental TL peak [48,49,51].

The calculated curve which provides the best match with the experimental curve is indicated in Figure 8 by the squares. This was the only curve which could be matched in part with the TL peak indicated

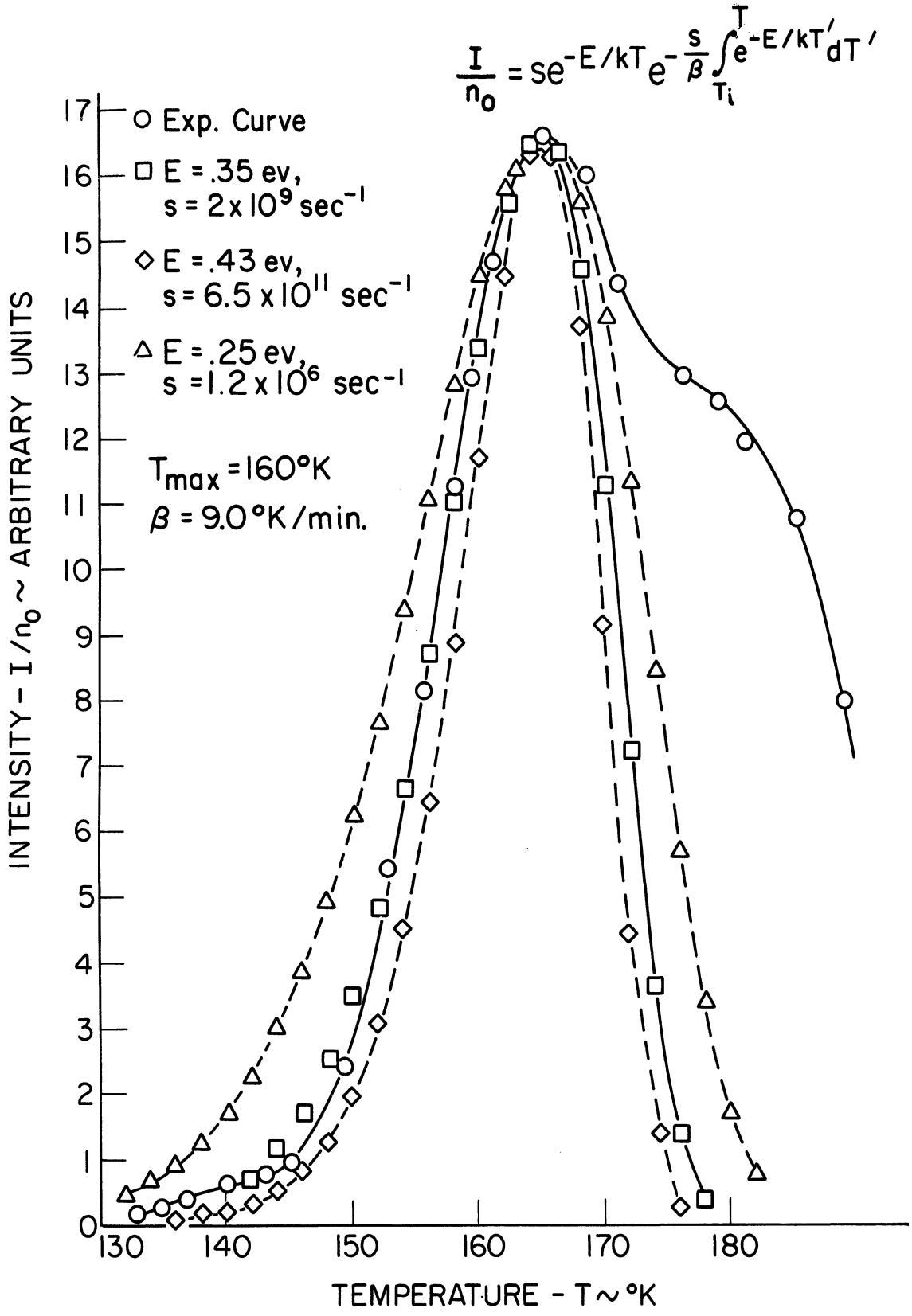

Figure 8

Application of Randall-Wilkins' Equation to First TL Peak of Nominally Pure $CaWO_4$

by the circles. A proper fit between both curves was obtained only for the low temperature side of the TL peak, since it was possible to eliminate the small intensity peak at 135°K mentioned in section 2.3, by heating to 145°K and subsequent cooling. However, this method of removing TL peaks by partial annealing can not be applied to the additional peak observed at 175°K (section 2.3), since it would also remove the major TL peak at 160°K. The values of the trap depth and the frequency factor corresponding to the best match between the calculated curve and the experimental peak are 0.35 ev and 2×10^9 sec^{-1} respectively.

It will now be shown that the same value of the frequency factor can be obtained by using the trap depth of 0.35 ev in Vasileff's expression[56]. This expression is indicated by equation (15) in Appendix II; i.e.:

$$s(E, T_{eff}) = P(E, T_{eff}) \exp(E/kT_{eff}) \tag{15}$$

This equation relates the energy and temperature dependent frequency factor $s(E, T_{eff})$ to the ionization rate $P(E, T_{eff})$ and the trap energy E. The parameters T_{eff} and k are the effective TL peak temperature and Boltzmann's constant respectively. Vasileff has shown that the theory of thermal ionization of trapped electrons in polar crystals predicts an energy and temperature dependent frequency factor[55], whereas Randall and Wilkins assumed that the frequency factor is independent of energy and temperature. The trapped electron is considered in this theory to be at an interstitial position between two unlike ions. These two ions and the trapped electron can be represented by a diatomic model. Upon heating of the crystal, energy is transferred from the lattice to

the trapped electron. This energy is attributed to phonons (p) with frequency (ω_ℓ) characteristic of the logitudinal vibrations of the lattice at the trapping center. An energy transfer ($p\omega_\ell\hbar$) equal to the trap depth (E) caused the thermal ionization of the trapped electron. This ionization was associated with a multiple phonon absorption by the interstitially trapped electron.

Equation (15) was used to calculate the energy and temperature dependent frequency factor of the first TL peak of pure $CaWO_4$ corresponding to a trap depth of 0.35 ev and an effective peak temperature of 155°K. The effective TL peak temperature was considered since equation (15) does not include the heating rate. It was assumed in this calculation that the electron was trapped at an interstitial position between the calcium ion and the tungstate radical. The four oxygen atoms of the tungstate radical were placed at the tungsten site to define a diatomic system consisting of two unlike ions. The volume (V) associated with this diatomic system was found by comparison with a structural model of a $CaWO_4$ crystal to be one-fourth of a unit cell (7.81×10^{-23} cm^3). The mass (M) corresponding to this volume was that of one $CaWO_4$ molecule (5.74×10^{-23} gm).

The transverse vibrational frequency (ω_t) of the $CaWO_4$ lattice at the interstitial trapping center was obtained from the first order Raman spectrum of $CaWO_4$ reported by Russell and Louden[29], and Porto and Scott[30] (4.6×10^{13} c/sec). This frequency (ω_t) and the static (ε_o =8.0) and high-frequency (ε_∞ =3.6) dielectric constants were used to calculate the corresponding longitudinal vibrational frequency (ω_ℓ = 6.86×10^{13} c/sec) from

$$\omega_\ell = \omega_t \left(\varepsilon_o/\varepsilon_\infty\right)^{1/2}$$

The effective mass (m*) of an electron in the conduction band of $CaWO_4$ was assumed to be equal to the free electron mass (9.108×10^{-28} gm), because no experimental information was available.

These constants are summarized in Appendix II together with the calculated quantities necessary for the numerical solution of equation (15). The frequency factor corresponding to a trap depth E=0.35 ev and a temperature T_{eff}=155°K was found from this calculation to be 4.36×10^{9} sec^{-1}. This value is in good agreement with the frequency factor of 2×10^{9} sec^{-1} obtained with Randall's equation for the same trap depth E and temperature T_{max}=160±5°K.

The method to be described now for finding the trap depth and the energy and temperature dependent frequency factor makes use of equations (8) and (15) shown above. The advantages of this method are that it eliminates the need for fitting the curve calculated with equation (6) to the experimental TL peak and that it provides temperature and energy dependent frequency factor values.

The peak temperature and corresponding heating rate of the three major TL peaks of pure $CaWO_4$, shown in Figure 5, were used in equation (8) to provide a relationship between the trap depth E and the temperature and energy independent frequency factor s. The straight lines of log(s) versus E obtained for each TL peak, are shown in Figure 9 together with the peak temperature (T_{max}) and heating rate (β). The experimental TL peak temperatures(T_{max}) were used and not the effective peak temperatures (T_{eff}) because equation (8) includes the heating rate. The position and the slope of these straight lines are not changed by small variations in T_{max} (±5°K) and β (±1°K/min). This was mentioned earlier with reference to the first TL peak shown in Figure 7.

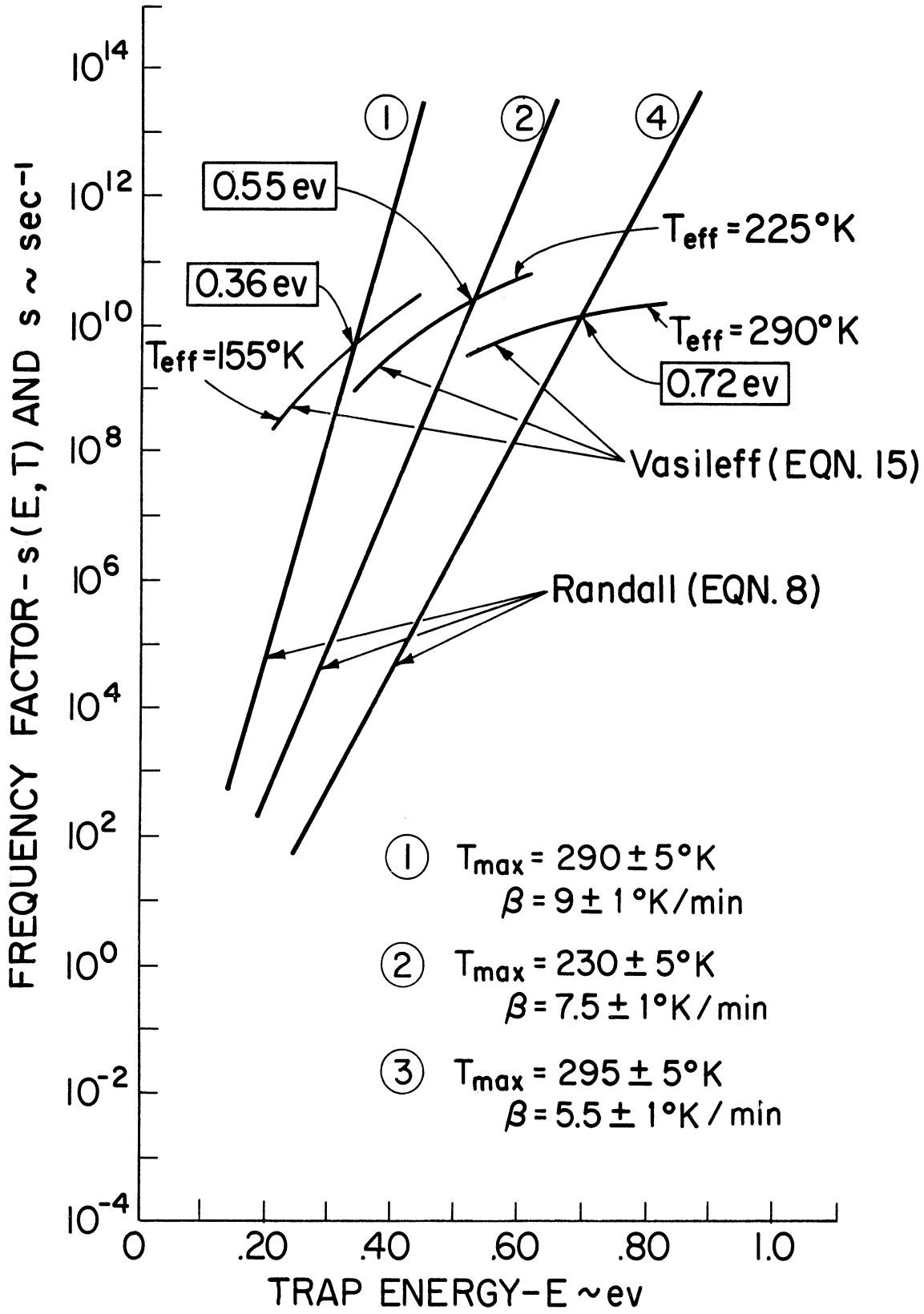

Figure 9

Trap Depth Determination of Three Major TL Peaks of Nominally Pure $CaWO_4$

The relationship between the energy and temperature dependent frequency factor $s(E,T_{eff})$ and the trap depth E was calculated from equation (15) using the constants listed in Appendix II. The resulting curves of $\log(s(E,T_{eff}))$ versus E are shown in Figure 9 for the three major TL peaks of pure $CaWO_4$ at the effective peak temperatures of 155°K, 225°K, and 290°K. The effective TL peak temperatures (T_{eff}) were used since Vasileff's equation does not include the heating rate. The calculated curves are indicated only in the region of intersection with the straight lines obtained from Randall's equation.

The values of the trap depth E and the energy and temperature dependent frequency factor s(E,T) were obtained from the point of intersection of the lines corresponding to the same TL peak. These values are summarized below for the first , second , and fourth TL peak.

	first peak	second peak	fourth peak
E ev	0.36±.02	0.55±.02	0.72±.02
$\text{Log}_{10}(s(E,T))\text{sec}^{-1}$	9.6±0.2	10.3±0.4	10.0±0.2

2.4 Discussion

The trap energy values of the three major TL peaks of pure $CaWO_4$ obtained with the described method, are compared in this section with those reported by Sayer and Souder[40] and with similar results obtained from the application of other commonly used methods to the experimental TL peaks.

The method discussed in section 2.3 for finding the trap energy and the frequency factor of the TL peaks makes use of Randall's and Vasileff's equation. Randall's equation can be solved for the number of

electrons (n*) remaining in the traps upon heating of the crystal to the TL peak temperature T_{max} and subsequent recooling. The number of electrons remaining in the traps is given by equation (12) in Appendix I; i.e.:

$$n^* = n_o \exp\left(-1\right) \tag{12}$$

Here, n_o refers to the original number of electrons in the traps before heating. This equation predicts that 1/e of the original number of electrons remain in the traps after heating of the sample to the TL peak temperature T_{max}. Since the derivation of Randall's equation assumed that the TL intensity (I) is directly proportional to the number of electrons (n) remaining in the traps at temperature T

$$I = n s \exp\left(-E/kT\right)$$

it is possible to provide experimental evidence of the number of trapped electrons at T_{max} by repeated cyclic heating of the sample to the TL peak temperature and by forming the ratios of the resulting TL peak intensities. Two such experimental intensity ratios (I_2/I_1; I_3/I_1) are shown below for the three major TL peaks of pure $CaWO_4$.

	Equation (12) Apendix I	First Peak	Second Peak	Fourth Peak
$\frac{I_2}{I_1}$	0.368	0.40	0.46	0.33
$\frac{I_3}{I_1}$	0.135	0.11	0.12	0.16

Here, the first TL peak intensity (I_1) is normalized to one and the subscripts on I refer to the order of preheating. Also indicated are the two corresponding ratios of the number of electrons remaining in the traps to the original number of electrons, predicted by equation (12). Good agreement is obtained between these predicted values and the experimental results despite the difficulties encountered in stopping the heating cycle exactly at T_{max}. This agreement provided supporting evidence for applying Randall's equation to the three major TL peaks of pure $CaWO_4$.

The trap energy and effective TL peak temperature values of the three significant TL peaks obtained in this investigation, are summarized below in row a. Also indicated in row b are the corresponding values reported by Sayer and Souder[40] for gamma-irradiated pure $CaWO_4$. A

TL PEAK		EFFECTIVE PEAK TEMP. (°K)	TRAP ENERGY (ev)
FIRST	a	155±3	0.36±.02
	b	160±5	0.32±.03
SECOND	a	225±3	0.55±.02
	b	219±19	0.44±.03
FOURTH	a	290±3	0.72±.02
	b	305±15	0.62±.03

comparison of the peak temperature values in the second column indicates that the same TL peaks are reported. Although the trap depth values in the third column are in reasonable agreement, it is interesting to note that the trap depths reported by Sayer and Souder especially for the higher temperature TL peaks, are always lower than the corresponding values obtained in this investigation. The reason for this is that Sayer and Souder evaluated the trap depth by a method which uses the slope of the low temperature side of the TL curve. It has been mentioned in section 2.3 that an experimental TL peak usually contains additional small intensity peaks which cause a broadening of the major TL peak. This increase in the half-width will reduce the slope of the low temperature side of the TL curve and thus result in reduced values of the trap energy. A similar conclusion was drawn from the TL curves calculated from Randall's equation and shown in Figure 8. It was observed then that a broadening of the major TL peak will result in reduced trap depth values.

The average values* of the trap depth E and frequency factor s obtained from the application of other commonly used methods to the three major TL peaks of pure $CaWO_4$, are summarized in Table II. The first row shows the values of E and s (E,T) determined by the present method. The last row indicates the mean of all calculated values of the trap depth and frequency factor. The equations used for the determination of E and s are enumerated in the first column. The methods of applying these equations to the experimental TL peaks are discussed in Appendix III.

The relatively large scatter of the trap depths E and the frequency

---

* The average value for any one trap is a mean of between five and ten determinations of the parameters of that particular trap

TABLE II

AVERAGE VALUES OF TRAP DEPTHS AND FREQUENCY FACTORS OF THREE MAJOR TL PEAKS OF NOMINALLY PURE $CaWO_4$

EQUATIONS / METHODS		FIRST PEAK		SECOND PEAK		FOURTH PEAK	
		E (ev)	$\log_{10}(s)$	E (ev)	$\log_{10}(s)$	E (ev)	$\log_{10}(s)$
PRESENT METHOD		0.36 ± .02	9.6±.2	0.55 ±.02	10.3±.4	0.72 ±.02	10.0 ± .2
$\frac{I}{n_0} = s \exp\left(-\frac{E}{kT}\right)\exp\left(-\frac{E}{\beta}\int_{T_i}^{T}\exp\left[-\frac{E}{kT'}\right]dT'\right)$ REF (46)		0.35 ± .03	9.3±.2	0.5 ± .03	9.2±.2	0.7 ± .03	9.8 ± .2
$E = k\left[T_{max_2}^{-1} - T_{max_1}^{-1}\right] \ln\left[\frac{\beta_1 T_{max_2}^2}{\beta_2 T_{max_1}^2}\right]$		0.11 ± .03		0.3 ± .04		0.48 ± .08	
$s = \frac{\beta}{T_{max}} \frac{E}{kT_{max}} \exp\left[\frac{E}{kT_{max}}\right]$ REF (46)			1.48±1.1		5.3±.7		5.2 ±1.8
$E = 1.51 kT_1 T_{max}\left[T_{max} - T_1\right]$		0.35 ± .05		0.42 ± .02		0.8 ± .05	
$s = 3\beta T_1 \exp\left[\frac{E}{kT_{max}}\right]\left(2T_{max}\left[T_{max} - T_1\right]\right)^{-1}$ REF (48)			10 ± 1.4		7.6 ± .3		11.3 ± 1.0
$E = T_{max}/408$ REF (49)		0.38 ± .03		0.54 ± .03		0.74 ± .03	
$E = kT_1 T_2 (T_2 - T_1)^{-1} \ln(I_2/I_1)$ REF (50)		0.28 ± .04		0.33 ± .07		0.69 ± .09	
$E = kT_{max}^2 \delta_m^{-1}$		0.14 ± .02		0.36 ± .03		0.5 ± .09	
$s = \beta \delta_m^{-1} \exp(T_{max}/\delta_m)$ REF (51)			2.1 ± .9		5.3±1.0		5.9 ± 1.9
$I \propto \exp\left(-\frac{E}{kT}\right)$	LOW TEMPERATURE (BEFORE PREHEAT)	0.36 ± .03		0.29 ± .04		1.01 ± .03	
	(AFTER PREHEAT)	0.36 ± .02		0.55 ± .02		0.75 ± .12	
	HIGH TEMPERATURE			0.66 ± .04		1.3 ± .30	
$\ln\left(\frac{A_t}{I(t)}\right) = \frac{E}{kT} - \ln(s)$ REF (52,53)		0.37 ± .04	10.9 ± .9	0.48 ± .10	9.7 ± 2.0	1.1 ± .30	15.5 ± 4.5
MEAN VALUE		0.35	9.95	0.53	9.7	0.72	10.3

factor s corresponding to the same TL peak illustrates the failure of some, commonly used methods to yield reasonable* values of E and s. However, a comparison of the trap depths and the frequency factors obtained by the present method, with the mean, shows that the described method seems to provide satisfactory values of E and s.

This chapter presented a method for calculating the trap depth of the three major trapping centers in pure $CaWO_4$ and discussed the TL curves caused by the thermal release and recombination of single electrons from the traps. Since it is possible to observe these unpaired electrons in the traps with electron spin resonance measurements, additional information about the trapping centers is obtained by correlating both TL and ESR measurements. This will be described next.

---

* Reasonable refers to a comparison of each individual value with the mean corresponding to one TL peak

III ELECTRON SPIN RESONANCE

The ESR measurements on gamma-irradiated $CaWO_4$ are presented in this chapter. Three paramagnetic centers were observed in these crystals. The centers are identified and assigned to the three TL peaks after differential thermal annealing. These centers are discussed and compared with those of Zeldes and Livingston[60].

3.1 Introduction

Electron spin resonance was introduced in physics about 20 years ago for studying systems that possess unpaired electrons with their associated magnetic moments. Examples for such systems possessing unpaired electrons, are transition metal ions (unfilled d-shell) and the inner transition ions (unfilled f-shell). These unpaired electrons form paramagnetic centers.

ESR measurements involve induced transitions between the Zeemann levels of these paramagnetic centers. For instance, the lowest energy level of paramagnetic W^{+5} in gamma-irradiated $CaWO_4$ is two-fold degenerate in electronic spin S ($S = \frac{1}{2}$). This level splits into two ($M = \pm\frac{1}{2}$) when the sample is placed in a static magnetic field (Zeemann splitting). The energy separation between these levels is determined by the magnetic field H and given by $(g\mu_B H)$, where g and μ_B are the spectroscopic g-factor and the Bohr magneton respectively. Each level may split further into $(2I + 1)$ hyperfine components because of the interaction between the electron spin S and the nuclear spin I. The induced transitions may be described by the simplified spin Hamiltonian

$$\mathcal{H} = g\mu_B \vec{S} \cdot \vec{H} + A \vec{S} \cdot \vec{I}$$

where the first term represents the Zeemann splitting and the second term is the hyperfine interaction.

Transitions between these levels of similar nuclear orientation ($\Delta M_I = 0$) can be induced by photons of energy $h\nu$, where ν is usually kept constant and H is varied. Resonant transitions are then indicated by a net absorption of energy from the radiation field. The values of the resonant magnetic field and the number of absorption peaks and their separation as a function of crystal orientation provide information about the nuclear and electronic spins of the paramagnetic ions, their possible valence state and lattice site, and the crystal field symmetry. This information obtained from ESR measurements together with the ability to detect minute concentrations allow identification of the paramagnetic centers.

3.2 Experimental Procedure and Apparatus

Electron spin resonance measurements were performed on the same $CaWO_4$ crystals described in the previous chapter. The $CaWO_4$ samples were oriented by x-ray diffration and then cemented to the end of the quartz rods. To produce paramagnetic centers, these samples were gamma-irradiated at 78°K with the same cobalt-60 source discussed earlier. The irradiation time was varied from 2 minutes to 2 hours. After gamma-irradiation, the samples were inserted into the microwave cavity which was kept at 78°K. Extreme care was exercised to avoid heating of the crystals during this transfer. The quartz rod served as the rotational axis for changing the crystal orientation in the magnetic field.

The ESR spectra of the gamma-irradiated pure $CaWO_4$ samples were obtained before and after cyclic heating of the cavity to approximately

186°K, 246°K, and 350°K. The TL curves of pure $CaWO_4$ described in the previous chapter, showed that the three major TL peaks are consecutively eliminated at these temperatures. The ESR spectra were observed each time at 78°K to establish a common basis for comparison. Some ESR measurements were performed at temperatures below 78°K, if excessive broadening of the ESR spectrum occurred at 78°K.

The equipment for obtaining the ESR spectra was the same as that used by Chu and Kikuchi[63] in their study of oxygen vacancies produced by fast neutron irradiation of $CaWO_4$. An X-band, Varian spectrometer operating at 9.5 Gc/sec with 400 c/sec modulation together with a ceramic, cylindrical TE-001 microwave cavity with variable cross coupling loops were used for these measurements. The magnetic field H was provided by a twelve inch rotating electromagnetic with a 3.25 inch gap. The field was measured with a proton probe connected to a Varian F-85 fluxmeter. For more accurate measurements, a Berkeley 7800 transfer oscillator and a Berkeley 7370 Universal EPUT were connected also to the fluxmeter.

3.3 Experimental Results

This section describes the ESR spectra of unirradiated-and gamma-irradiated pure $CaWO_4$. Three paramagnetic centers produced by gamma-irradiation are identified and assigned to the three major TL peaks of $CaWO_4$ by differential thermal annealing.

Typical ESR spectra of unirradiated- and gamma-irradiated nominally pure $CaWO_4$ at 78°K, with the magnetic field parallel to the c-axis of the crystal, are shown in Figure 10.

The lower trace gives the ESR spectrum of $CaWO_4$ at 78°K observed before gamma-irradiation. The spectrum consisting of five sets of six

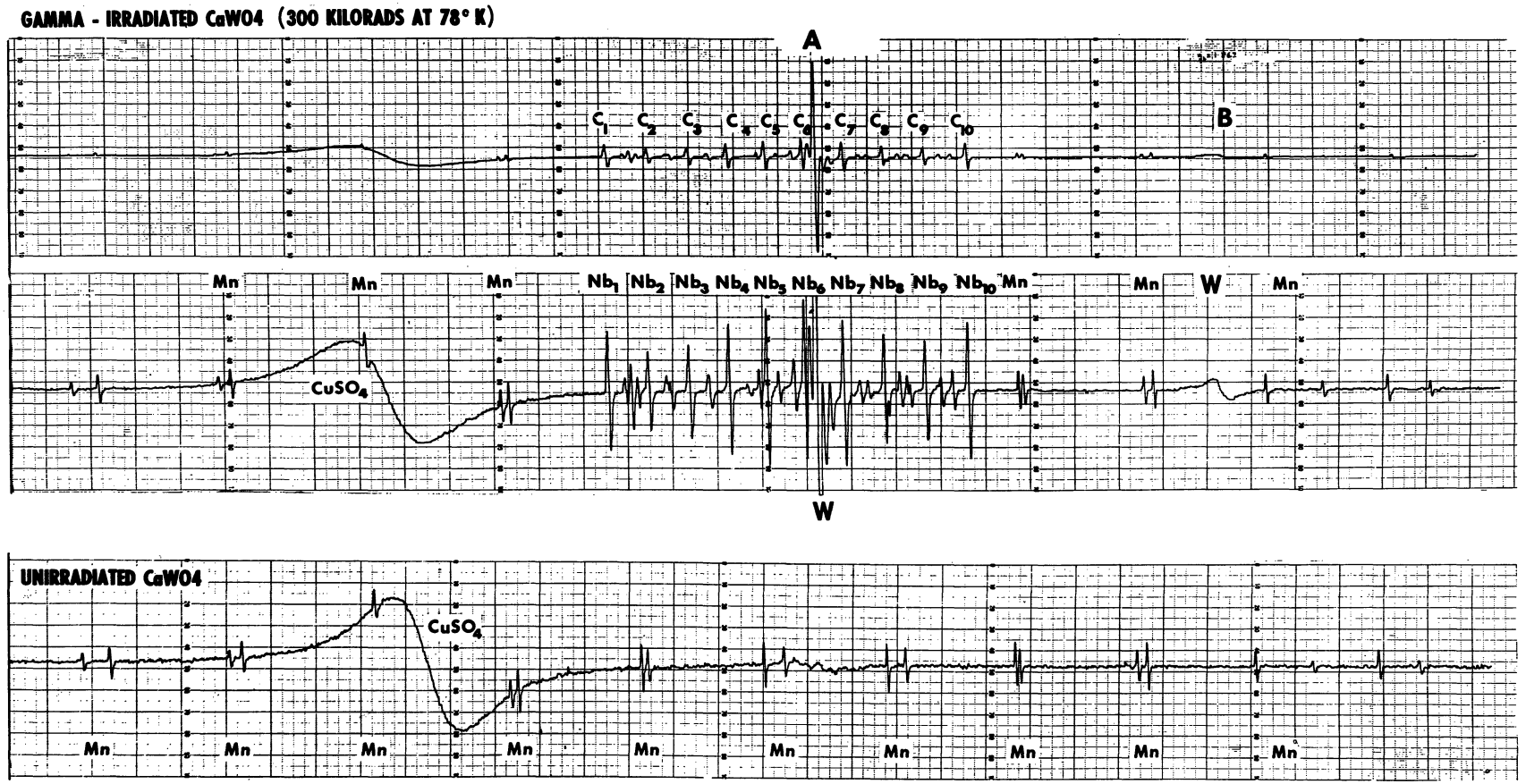

Figure 10

ESR Spectra of Gamma-irradiated and Unirradiated Pure $CaWO_4$ at 78°K. H Parallel to (001) Axis

lines when the magnetic field was parallel to the c-axis, was identified by Kedzie and Kestigian[19], and Hempstead and Bowers[64] as due to manganese (Mn^{+2}) in the calcium (Ca^{+2}) site. This unintended manganese impurity was common to all ESR spectra of $CaWO_4$ and was unaffected by the gamma-irradiation.

The upper two traces show the ESR spectra of $CaWO_4$ after gamma-irradiation of 300 kilorads at 78°K. Three new sets of lines were observed at 78°K. They were labeled as group A, group B, and group C as shown in the top trace. Because of the large difference in line intensities between these three groups, only group A is clearly visible in the upper trace. However, groups B and C are distinctly indicated in the second trace.

Group A consists of one strong central line with two lower intensity lines equally spaced on either side when the magnetic field is along the (001) direction. These three lines split into two sets of three lines with the magnetic field in the ab-plane. Four sets of three lines were observed when the magnetic field was in any other direction.

The experimentally determined g-values in the (001) and (110) direction and the hyperfine separation of the group A spectrum are summarized below together with the corresponding values reported by Zeldes and Livingston[60] for paramagnetic tungsten W^{+5} in gamma-irradiated $CaWO_4$.

	g_{001}	g_{110}	hyperfine separation
Present Work	2.009	2.0190	9.4 gauss
Zeldes and Livingston	2.009	2.0173	9.0 gauss

The similarity of these ESR results provides sufficient evidence that the same paramagnetic center was observed. Hence, the spectrum associated with group A was assigned to paramagnetic tungsten*.

Group C consists of ten lines approximately equal in intensity and spacing when the magnetic field is along the (001) direction. Again, two groups of ten lines were present with the magnetic field in the ab-plane and four sets of ten lines when the magnetic field was in any other direction. The experimental g-values in the (001) and (110) direction and the hyperfine separation of this niobium spectrum are indicated below together with the corresponding values reported by Chu and Kikuchi[3] for paramagnetic niobium Nb^{+4} in gamma-irradiated $CaWO_4$:Nb.

	g_{001}	g_{110}	hyperfine separation
Present Work	2.021	2.025	29-30 gauss
Chu and Kikuchi	2.023	2.026	29 gauss

The close correspondence of these ESR results provided convincing evidence that the same paramagnetic center was observed. For this reason, the spectrum associated with group C was assigned to paramagnetic niobium. The unexpected occurrence of niobium in all pure $CaWO_4$ samples is not too surprising, since there was a common supplier of the $CaWO_4$ powder which was used as the source material for the growth of the single crystals. The additional lines observed in the niobium ten-line spectrum are caused by forbidden transitions.

---

* Hereafter, $(W^{+5})_A$ will refer to this tungsten center

Group B consists of a single broad line which was resolved into a line spectrum only at temperatures below 78°K. The temperature dependence of group B is shown in Figure 11. The top trace indicates that the line spectrum of group B at 30°K consists of one strong central line and two lower intensity lines, equally spaced on either side, when the magnetic field is along the (001) direction. These three lines split into two sets of three lines with the magnetic field in the ab-plane. The experimentally determined g-values in the (001) and (110) direction and the hyperfine separation of the group B spectrum are summarized below together with the corresponding values reported by Zeldes and Livingston[60] for paramagnetic tungsten W^{+5} in gamma-irradiated $CaWO_4$.

	g_{001}	g_{110}	hyperfine separation
Present Work	1.843	1.605	50 gauss
Zeldes and Livingston	1.846	1.604	35-60 gauss

The similarity of these ESR results implied that the same paramagnetic center was observed. Hence, the spectrum associated with group B was assigned also to paramagnetic tungsten*.

No attempt was made to study the additional structure indicated within the paramagnetic tungsten $(W^{+5})_B$ spectrum at 30°K. It is clearly shown that this spectrum merges into the broad line at 80°K indicated in Figure 10.

The identification of the paramagnetic tungsten (W^{+5}) and niobium (Nb^{+4}) ions with the trapping centers responsible for the TL peaks of

---

* Hereafter, $(W^{+5})_B$ will refer to this tungsten center

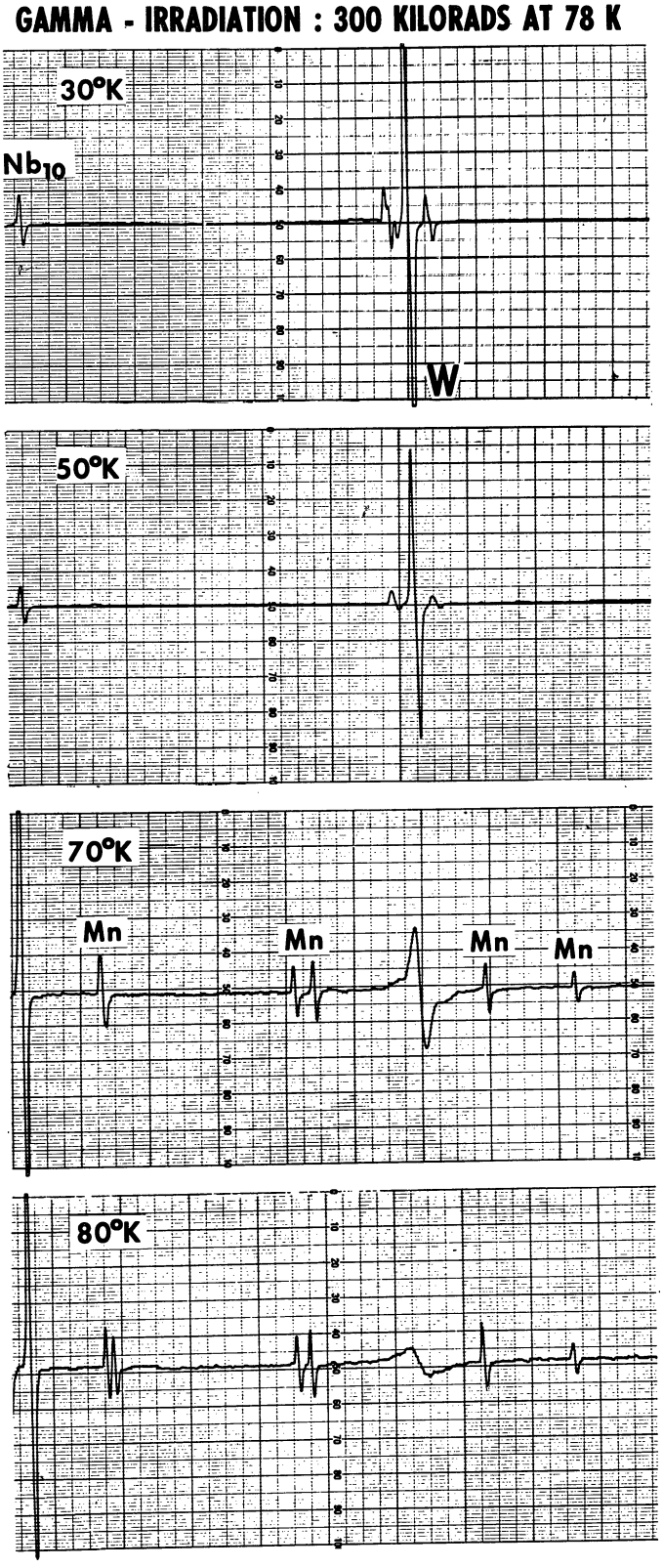

Figure 11

Temperature Dependence of Group B Spectrum of Gamma-irradiated Pure $CaWO_4$. H Parallel to (001) Axis

nominally pure $CaWO_4$, was made from observation of the ESR spectra after differential thermal annealing. This is illustrated in Figure 12.

The upper two traces give the ESR spectra of pure $CaWO_4$ after gamma-irradiation of 300 kilorads at 78°K. These traces show the three groups of lines A, B, and C, which were previously discussed and assigned to paramagnetic tungsten (W^{+5}) and niobium (Nb^{+4}) respectively.

The third trace shows that the first paramagnetic tungsten $(W^{+5})_A$ spectrum, labeled as group A, is no longer observed after the sample was heated to approximately 190°K and cooled to 78°K. The TL curve of pure $CaWO_4$ given in Figure 5 of Chapter II, indicated that the first TL peak is removed by such a heating cycle. This correlation was taken as evidence for identifying the $(W^{+5})_A$ ions with those trapping centers which are responsible for the first TL peak.

The fourth trace indicates that similar cyclic heating to approximately 250°K removed the second tungsten $(W^{+5})_B$ spectrum corresponding to group B. These $(W^{+5})_B$ ions are identified with the trapping centers causing the second TL peak, since TL measurements verified the removal of this peak by such a heating cycle.

The last trace shows that heating of the crystal to approximately 350°K removed the niobium (Nb^{+4}) spectrum associated with group C. The Niobium ions are identified with the trapping centers responsible for the fourth TL peak, since similar cyclic heating removed this TL peak.

The ESR spectrum given in the bottom trace is the same as that of unirradiated pure $CaWO_4$ shown in Figure 10.

The broad ESR absorption line of $CuSO_4$ indicated in all traces, was used as a standard for absolute intensity measurements of the ESR spectra, to investigate the influence of temperature and gamma-irradiation

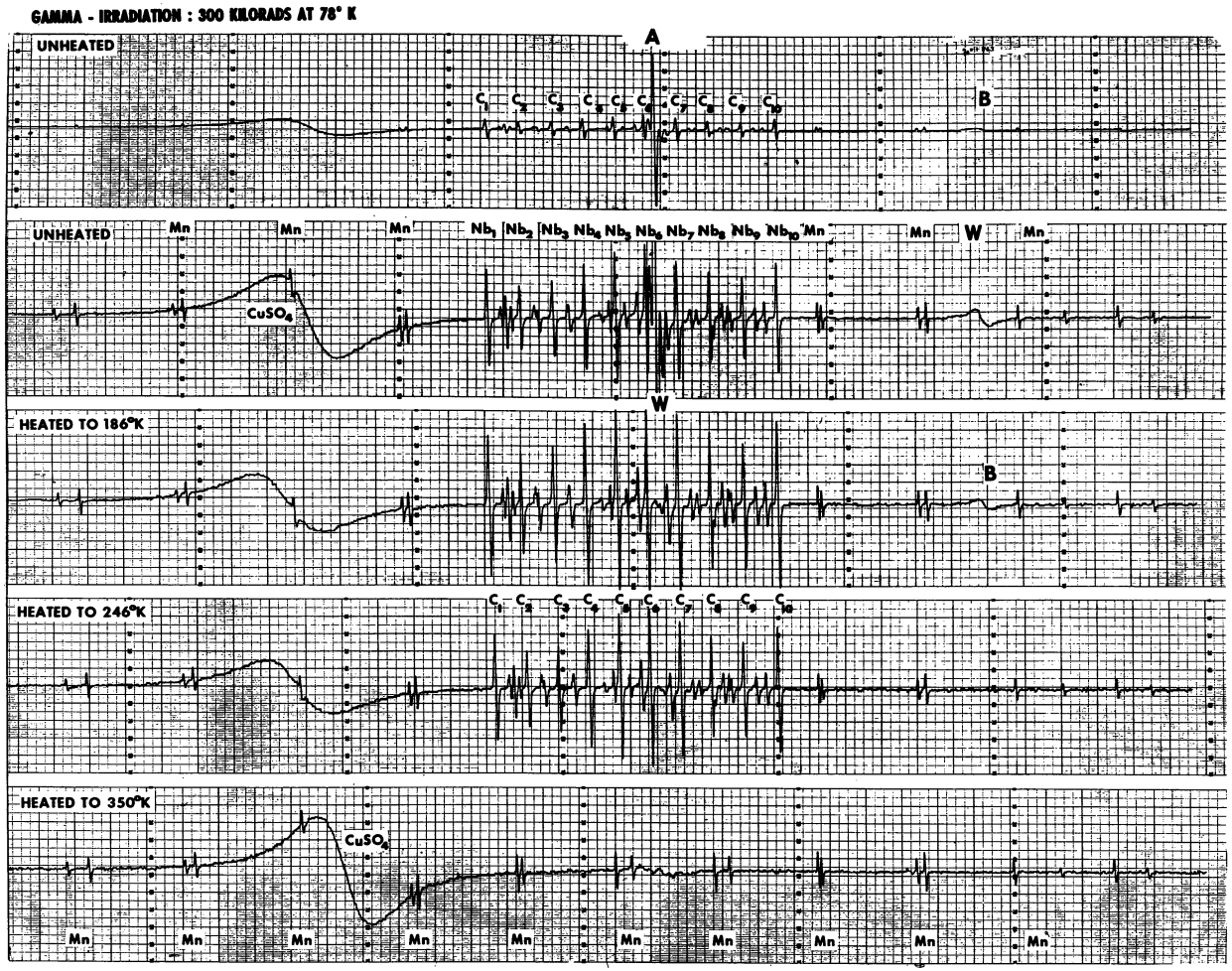

Figure 12

ESR Spectra of Gamma-irradiated Pure $CaWO_4$ at 78°K After Differential Thermal Annealing. H Parallel to (001) Axis

dose on the line intensities. This will be discussed in the following section.

3.4 Discussion

The ESR spectra of gamma-irradiated pure $CaWO_4$ obtained in this investigation are discussed and compared with those reported by Zeldes and Livingston[60].

Two paramagnetic tungsten centers were observed by the above investigators at 78°K in gamma-irradiated $CaWO_4$ crystals grown by the Verneuil flame-fusion process. It is shown in the previous section that these two centers are similar to those observed in this investigation of gamma-irradiated $CaWO_4$ samples, grown by the Czochralski method. The spectrum associated with $(W^{+5})_A$ was assigned by Zeldes and Livingston to electron deficient species containing two nearly equivalent tungsten ions on the basis of four hyperfine lines. The $(W^{+5})_B$ spectrum was attributed to a single tungsten ion with an extra electron. Both spectra were reported to disappear at the same rate and the same temperature (141°K).

This assignment of the two tungsten spectra disagrees with the results presented in section 3.3. Furthermore, if the paramagnetic centers were formed by correlated electron deficient and electron surplus centers, they would also saturate simultaneously upon gamma-irradiation. However, differential thermal annealing experiments[59] on $CaWO_4$ samples irradiated at different gamma dosages, indicated that the second tungsten spectrum $(W^{+5})_B$ saturated first. This is shown in Figure 13 by comparing the line intensities of the $(W^{+5})_A$ and $(W^{+5})_B$ spectra at different gamma flux levels below saturation. These results imply that the paramagnetic centers are apparently formed by independently trapped electrons.

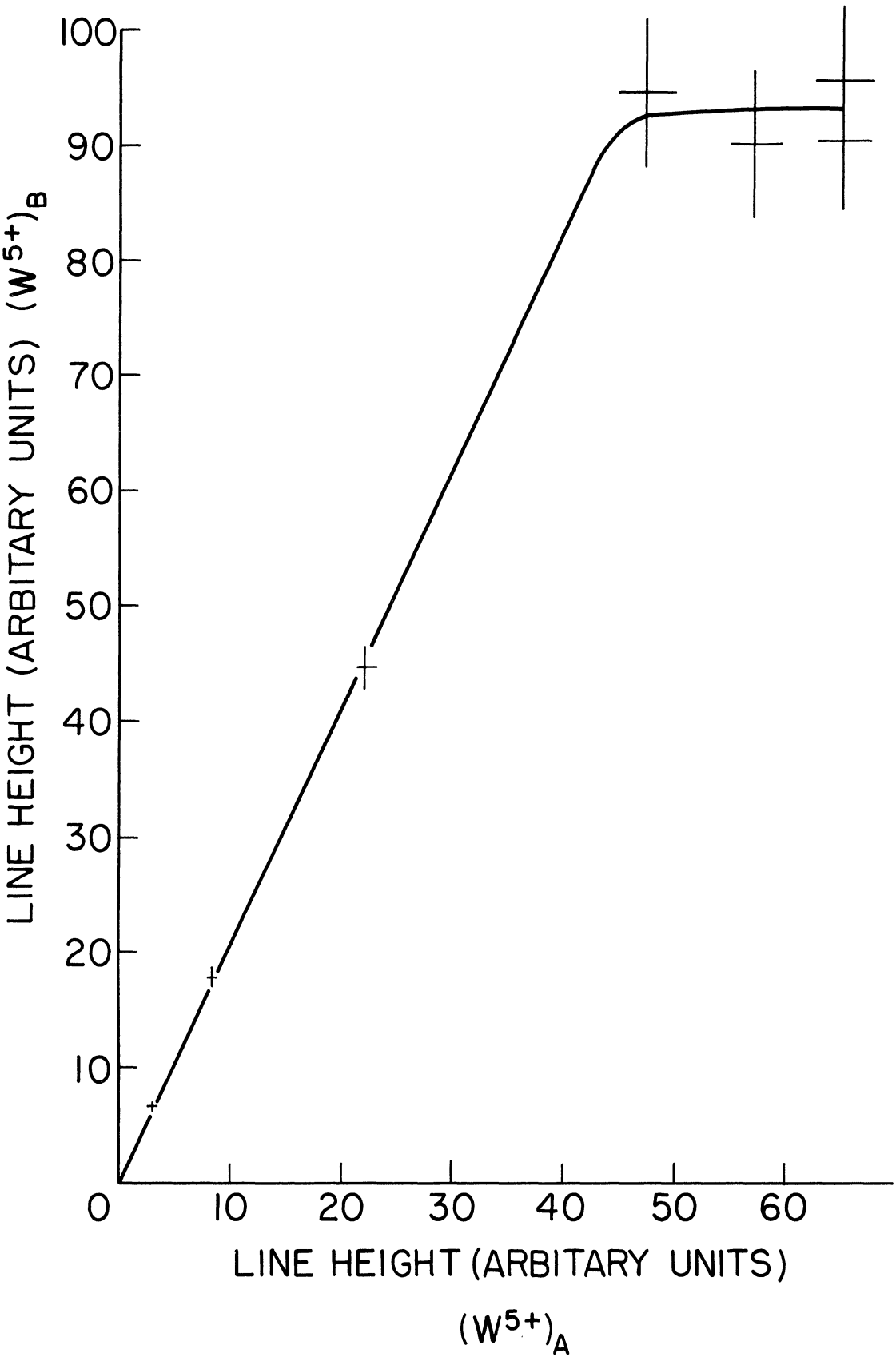

Figure 13

Comparative Saturation of First $(W^{+5})_A$ and Second $(W^{+5})_B$ Paramagnetic Tungsten Spectrum of Pure $CaWO_4$ at 78°K

Additional partial annealing experiments[59] on low flux (below saturation), gamma-irradiated pure $CaWO_4$ samples showed that the paramagnetic niobium (Nb^{+4}) concentration increased upon removal of the first tungsten $(W^{+5})_A$ spectrum. This was evidenced by an increase in the niobium line intensities. For instance, an increase by a factor of about two was observed after gamma-irradiation of 15 kilorads. This would indicate a transfer of electrons from the paramagnetic $(W^{+5})_A$ centers to the nonparamagnetic niobium (Nb^{+5}) ions; i.e. (Nb^{+5})appears to be more stable than $(W^{+5})_A$. Non-paramagnetic niobium (Nb^{+5}) centers were present in the $CaWO_4$ samples, since the niobium centers saturated at a higher gamma-irradiation dose than the $(W^{+5})_A$ centers. Figure 14 shows that the saturation of the paramagnetic $(W^{+5})_A$, $(W^{+5})_B$, and (Nb^{+4}) centers occurs at approximately 275 kilorads, 140 kilorads, and 550 kilorads respectively. Because of the relatively low intensity of the second tungsten $(W^{+5})_B$ spectrum it was not possible to observe a similar change in intensity.

Such a transfer of electrons can not be observed directly with TL, since the temperature at which the fourth TL peak occurs is such that the first two trapping centers are always empty. However, if the transfer of electrons to the trapping centers responsible for the fourth TL peak is associated with the emission of photons of energy equal to the trap depth then it should be possible to observe the retrapping of electrons by monitoring the wavelength of this emission @ 17240Å during TL of the first and second peak.

It was shown in this chapter that the trapping centers in nominally pure $CaWO_4$ responsible for the first two major TL peaks, can be identified with paramagnetic tungsten (W^{+5}) and the last TL peak with paramagnetic niobium (Nb^{+4}). This identification implied that the first and second

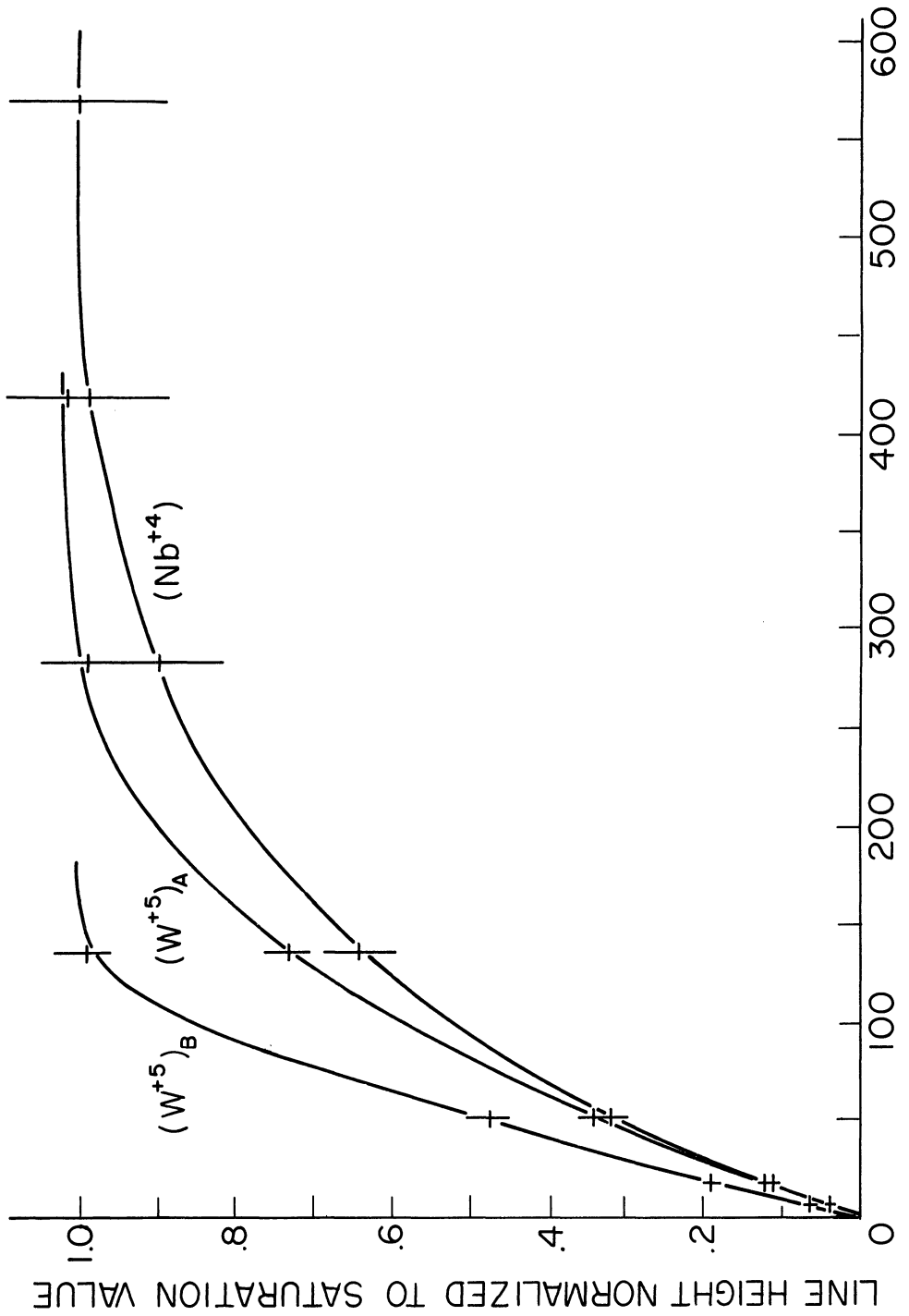

Figure 14

Saturation of Paramagnetic Tungsten and Niobium Centers upon Gamma-irradiation

TL peak are associated with lattice defects whereas the fourth TL peak is caused by impurities*. The next chapter will discuss some properties of the trapping centers which are useful for the assignment of these centers to particular lattice defects and impurities.

---

* It has been verified by TL and ESR measurements that paramagnetic vanadium (V^{+4}) and tantalum (Ta^{+4}) gives rise to similar trapping centers as the described niobium (Nb^{+4})

IV SUPPLEMENTAL EXPERIMENTS

Two trapping centers in charge compensated and uncompensated $CaWO_4:RE^{+3}$ are shown to be similar to those observed in pure $CaWO_4$. The density of these trapping centers is then determined and the influence of optical sources on the trap density discussed.

4.1 Thermoluminescence Curves of Doped $CaWO_4$

This section shows that the TL curves of trivalent samarium (Sm^{+3}) and terbium (Tb^{+3}) doped $CaWO_4$, and terbium charge compensated with pentavalent tantalum (Ta^{+5}) and vanadium (V^{+5}) doped $CaWO_4$* are similar to those obtained with pure $CaWO_4$.

Typical TL curves of Sm^{+3} and Tb^{+3} doped $CaWO_4$ after gamma-irradiation of 300 kilorads at 78°K are presented in Figure 15. Two major TL peaks were observed at approximately 235°K and 290°K with both crystals. The TL curve of nominally pure $CaWO_4$ was included to provide a basis for comparison. This curve was shown in Figure 5 and discussed in section 2.3. The TL curves of the 1% Sm^{+3} and 0.5% Tb^{+3} doped $CaWO_4$** crystals were monitored at the maximum TL emission intensity of 5640Å and 5430Å respectively. The 5640Å emission corresponds to the $^4G_{7/2} \rightarrow {}^6H_{9/2}$, $^4F_{3/2} \rightarrow {}^6H_{7/2}$, or $^4G_{5/2} \rightarrow {}^6H_{5/2}$ transition of Sm^{+3} in $CaWO_4$.

---

* Rare earth ions (except europium) enter $CaWO_4$ in the trivalent oxidation states $(RE)_2O_3$. These RE ions (radii 0.85Å to 1.14Å) are expected to prefer the calcium (Ca^{+2}) site (0.99Å) to the tungsten (W^{+6}) site (0.62Å). Charge compensation by a second ion is generally required to avoid lattice vacancies and distortions created by the RE ions. Vanadium (V^{+5}), niobium (Nb^{+5}), and tantalum (Ta^{+5}) ions in the form of $(V,Nb,Ta)_2O_5$ can be used for this purpose

** The concentration of the RE ions refers to the atomic percentage in the melt; i.e. the number of ions per hundred calcium (Ca^{+2}) or tungsten (W^{+6}) ions

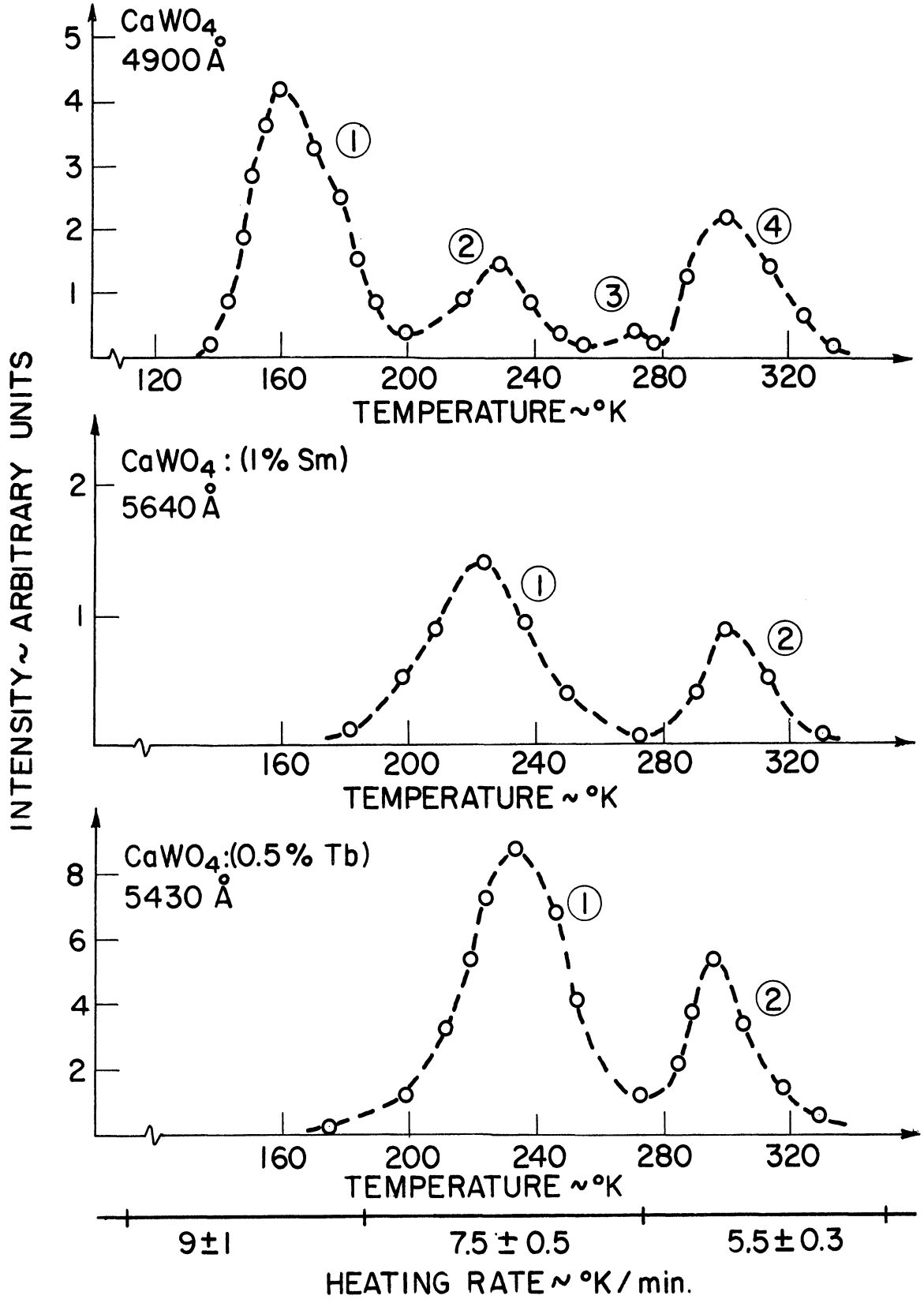

Figure 15

Typical TL Curves of $CaWO_4$ Doped With Samarium and Terbium After Gamma-irradiation of 300 Kilorads at 78°K

This indicates that when calcium tungstate is doped with a rare earth ion the TL spectrum is predominantly determined by the emission spectrum of the particular ion chosen.

It can be seen from Figure 15 that the first and second TL peak temperatures of the RE ion doped $CaWO_4$ samples were similar to the second and fourth TL peak temperatures of pure $CaWO_4$ respectively. This correspondence in peak temperature suggested that the same trapping centers were present in the doped and undoped $CaWO_4$ crystals. However, the relative intensity of these two TL peaks varied for the doped and undoped samples; i.e. the first TL peak was always larger than the second TL peak in $CaWO_4:RE^{+3}$ and smaller in pure $CaWO_4$. The largest luminescence yield was obtained with $CaWO_4:Tb^{+3}$. Only weak TL was observed with $CaWO_4:Sm^{+3}$.

It is further illustrated in Figure 15 that the first TL peak observed in pure $CaWO_4$ at approximately 160°K was not present in the RE^{+3} ion doped $CaWO_4$ crystals. The removal of this first TL peak upon RE^{+3} ion doping was confirmed by the absence of the $(W^{+5})_A$ lines from the ESR spectra of $CaWO_4:RE^{+3}$.

The influence of pentavalent charge compensators (V^{+5}, Ta^{+5}) on the TL curves of $CaWO_4:Tb^{+3}$ is shown in Figure 16. These TL curves were recorded at the maximum TL emission intensity of 5430Å. The TL curve of uncompensated Tb^{+3} doped $CaWO_4$ was included to provide a basis for comparison. This comparison of compensated and uncompensated Tb^{+3} shows that the presence of tantalum and vanadium does not affect the peak temperature of the first and second TL peak observed at approximately 235°K and 290°K respectively. However, the relative intensity of the TL peaks varied for charge compensated and uncompensated crystals; i.e. the

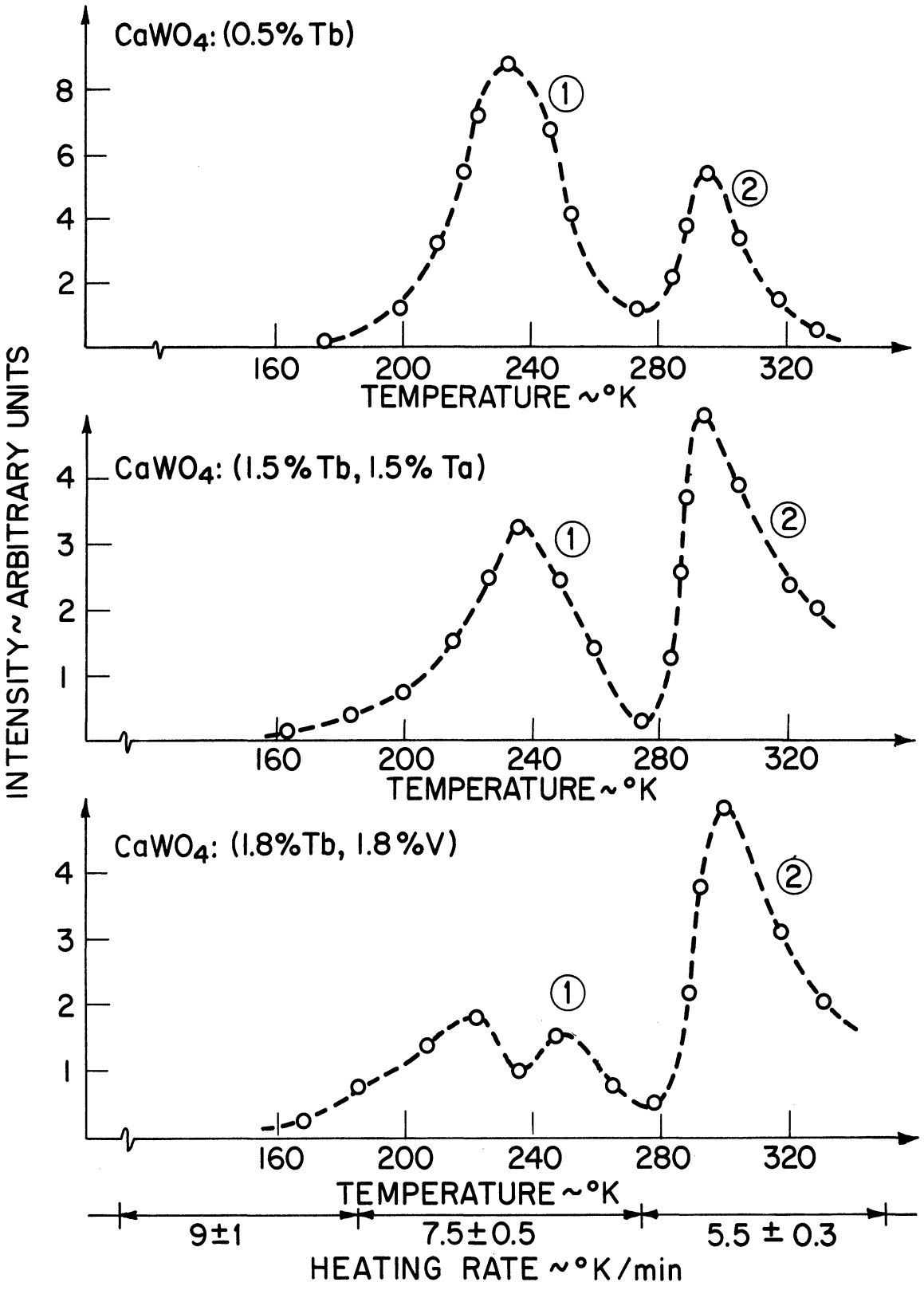

Figure 16

Typical TL Curves of $CaWO_4$ Doped With Terbium and Vanadium or Tantalum After Gamma-irradiation of 300 Kilorads at 78°K Emission Monitored at 5430Å

second TL peak was larger than the first TL peak in the compensated samples and smaller in the uncompensated crystals. This shift in the relative intensities of the TL peaks is not surprising since the second TL peak is attributed to paramagnetic Nb^{+4} in the tungsten site. Niobium is found in column VB of the periodic table together with vanadium and tantalum. These ions with a normal valence state of +5 are generally used as charge compensators in RE^{+3} ion doped $CaWO_4$ crystals. Therefore, it is not surprising that these ions produce similar effects on the TL curves of $CaWO_4:RE^{+3}$. Such effects were observed in the form of an increased second TL peak upon compensating with vanadium* and tantalum. Furthermore, the TL peak due to vanadium or tantalum occurs at a slightly higher temperature than the second TL peak due to niobium. This is evidenced by the relatively strong TL still observed at 320°K which left the crystals discolored at 350°K, and by preliminary ESR measurements of paramagnetic tantalum (Ta^{+4}) in $CaWO_4$**.

Figure 16 also illustrates that the TL peak observed in pure $CaWO_4$ at approximately 160°K was absent in the TL curves of charge compensated, rare earth ion doped $CaWO_4$ crystals.

4.2 Density of Trapping Centers in Pure $CaWO_4$

This section describes briefly the evidence for the natural occurrence of the trapping centers and the results of the trap density measurements.

---

* Paramagnetic vanadium (V^{+4}) in the tungsten site (group A) has been observed by Mahootian[35] (g_{001}=2.0245; $\langle A \rangle$ =19.7 gauss) and identified with the fourth TL peak in pure $CaWO_4$ by Mason (private communication)

** A paramagnetic tantalum (Ta^{+4}) spectrum which could be removed at approximately 310°K was observed by Mason and Irizarry-Milan in gamma-irradiated pure $CaWO_4$ and assigned to the tungsten site (private communication)

It is generally assumed that the energy loss of gamma-rays takes place primarily by ionization i.e. no additional electron traps are formed. Supporting evidence that irradiation of the $CaWO_4$ samples by gamma-rays filled only the naturally occurring traps was obtained from the saturation of the trapping centers. Absolute intensity measurements of the ESR spectra of the paramagnetic tungsten (W^{+5}) ions provided information about the saturation of the trapping sites which are responsible for the first and second TL peak of nominally pure $CaWO_4$. Saturation of these traps occurred for a typical sample size of 4x4x2 mm^3 at a gamma-irradiation dose of approximately 275 and 140 kilorads respectively (Figure 14). The trapping centers responsible for the fourth TL peak of nominally pure $CaWO_4$ saturated at approximately 550 kilorads. Using an average total gamma absorption coefficient[3] of 0.36 cm^{-1} and a gamma flux of 10^{13} gammas/second at the crystal position in the center well of the cobalt-60 source, the total number of gammas absorbed by the sample was estimated as 10^{16}.

The observation that similar TL curves can be obtained with doped and undoped $CaWO_4$ crystals (section 4.1) supports further the assumption of the natural occurrence of the trapping centers in pure $CaWO_4$.

An estimate of the density of the three major electron traps in $CaWO_4$ was obtained from TL measurements by assuming a one to one correspondence between the number of photons emitted and the number of electrons trapped and subsequently released upon heating. The retrapping of electrons is assumed to be negligible. The total area underneath each TL peak (intensity versus time) was found by graphical integration

and converted to number of photons by using the calibration constant* discussed in section 2.2. The first TL peak corresponds to approximately 10^{16} photons, whereas the second and fourth TL peak is due to about 10^{14} and 10^{15} photons respectively. Thus, all three major TL peaks of pure $CaWO_4$ contained approximately $10^{15\pm1}$ photons. For a typical $CaWO_4$ sample of 0.1 to 0.2 gm, the corresponding density of the trapping centers responsible for the three significant TL peaks was found to be about $10^{16\pm1}$ traps/gm (photons/gm). This value compared favorably with the trap density of approximately $10^{17\pm1}$ traps/gm obtained from ESR measurements by assuming a one to one correspondence between the spin concentration and the trapped electron concentration. $CuSO_4.5H_2O$ in single crystal form was used as a reference sample of known Cu^{+2} spin concentration. The density of the trapping centers (N_W) responsible for the first TL peak of pure $CaWO_4$ was obtained from the following expression**

$$N_W = \left(\frac{A_W}{A_{Cu}}\right)\left(\frac{g_{Cu}}{g_W}\right)^3 \frac{N_{Cu}}{\eta M_{CaWO_4}}$$

Where

$$N_{Cu} = \frac{M_{CuSO_4}\,(\text{Avogadro's number})}{(\text{mol. wt. of } CuSO_4 \cdot 5H_2O)}$$

In this equation, A_W and A_{Cu} represent the area underneath the $(W^{+5})_A$ and Cu^{+2} ESR absorption lines respectively, g_W and g_{Cu} the corresponding g_{001}-values of 2.009 and 2.230 respectively, M the weight of the

---

* This value was corrected for the spectral response of the system at the wavelength of the TL observation and for the geometry relation between the sample and the monochrometer entrance slit

** This expression is similar to a formula described and used by Chu[67] to calculate the total number of tungsten gamma centers in fast neutron-irradiated $CaWO_4$

samples, and η the isotopic abundance of the paramagnetic tungsten species in $CaWO_4$. Using this relation the total number of $(W^{+5})_A$ centers in $CaWO_4$ was found to be about 10^{18} traps/gm (spins/gm)*. A similar calculation of $(W^{+5})_B$ and Nb^{+4} centers resulted in approximately 10^{16} and 10^{17} traps/gm respectively. Thus, all three centers have approximately $10^{17\pm1}$ traps/gm.

4.3 Effect of Optical Radiation on Trap Density

This section describes briefly the influence of optical radiation on gamma-irradiated doped and undoped $CaWO_4$ at 78°K.

Broad band infrared (IR) radiation (0.2 ev to 0.8 ev) from a nichrome heater coil at 700°K caused a nearly uniform decrease in intensity of the major TL peaks of gamma-irradiated doped and undoped $CaWO_4$. During the irradiation process, the sample was maintained at 78°K. Emission of luminescence was observed as a result of the irradiation. This investigation of IR bleaching of the electron traps was performed in view of the possible use of the luminescence process for infrared detection. For instance, weak emission at 5430Å was induced by the infrared radiation in $CaWO_4$:Tb^{+3} at 78°K after the sample was gamma-irradiated by a 30 millicurie cobalt-60 source. This source was placed 10 cm from the sample in the dewar. The resulting gamma flux at the crystal was approximately 10^7 gammas/hour. An increase in emission was observed by using a 300 millicurie source at 1 cm distance from the sample resulting in a gamma flux of about 10^{12} gammas/hour at the crystal position. In the absence of IR radiation, no fluorescence was visible at 78°K independent of the gamma-irradiation dosage.

---

* Zeldes and Livingston[60] reported an average value of 2.5×10^{17} traps/gm

However, if during the process of gamma-irradiation at low intensity the luminescence of the sample is monitored, it is found that emission occurs only in the presence of IR. Some of the advantages which could be realized by an IR detector utilizing this effect may be compactness (nuclear pump), selection of narrow band IR detection capability (different trapping levels), and matching of the emission spectrum to maximum spectral response of the photodetector. The major disadvantage of such a system would be the reduced temperature at which the system must be operated.

Visible radiation (1.5 ev to 2.5 ev) from a 100 watt tungsten microscope lamp with the infrared light filtered out was focused on the gamma-irradiated samples at 78°K. The radiation produced a nearly uniform decrease in intensity of the three major TL peaks in pure $CaWO_4$. This observation is contrary to that of Zeldes and Livingston[60] who reported the disappearance of the $(W^{+5})_A$ centers and a weakened $(W^{+5})_B$ spectrum under similar experimental conditions. The opaque and black, gamma-irradiated samples bleached during optical irradiation.

Ultraviolet (UV) radiation (3.4 ev) from a 100 watt high pressure mercury lamp with visible and infrared light filtered out, was focused on the samples maintained at 78°K. This produced a slight decrease of the lowest temperature TL peak of pure $CaWO_4$ occurring at about 155°K. No such reduction in TL peak intensity was observed for the two high temperature TL peaks of pure $CaWO_4$. Similarily, no reduction of the corresponding TL peaks was observed in terbium and samarium doped CaWO4 (Figure 15).

A sample of $CaWO_4$:Tb maintained at 78°K was irradiated with UV. Upon subsequent heating it was found that a weak TL peak occurring near 225°K had been induced. The reason for not observing a similar

TL peak in $CaWO_4$:Sm and pure $CaWO_4$ may be the high luminescence efficiency of the terbium ions in $CaWO_4$ as compared to the samarium ions and pure $CaWO_4$*. An indication of the relative luminescence efficiency can be obtained from the TL yield observed with these crystals (Figure 15).

Some of the information contained in this chapter will be helpful in the assignment of defect models to the trapping centers discussed in the next chapter.

---

* Zeldes and Livingston reported a small concentration of the $(W^{+5})_A$ centers produced by UV light in pure $CaWO_4$ crystals at 78°K

V ASSIGNMENT OF DEFECT MODELS TO TRAPPING CENTERS

Three trapping centers responsible for the first, second, and fourth TL peak are described in this chapter. The impurity center identified with the paramagnetic niobium (Nb^{+4}) ion is discussed. Models for the lattice defects assigned to the paramagnetic tungsten $(W^{+5})_A$ and $(W^{+5})_B$ ions are proposed.

5.1 Crystal Structure of $CaWO_4$ and WO_3

This section gives a brief description of the crystal structure of $CaWO_4$ which is helpful in the interpretation of the lattice defects. The possible substitution of tungsten trioxide (WO_3) for WO_4^{-2} in $CaWO_4$ is discussed next, since WO_3 seems to be responsible for the tungsten $(W^{+5})_A$ and $(W^{+5})_B$ centers.

The scheelite crystal structure of $CaWO_4$ is characterized by the space group C_{4h}^6 or the tetragonal $I4_1/a$ with four molecules in the unit cell. The unit cell and its dimensions are shown in Figure 17. Each molecule is formed by tungsten (W^{+6}) , calcium (Ca^{+2}), and oxygen (O^{-2}) ions. The tungsten ion is covalently bonded to four oxygen ions in the form of a distorted (WO_4^{-2}) tetrahedron. The calcium ions are surrounded each by eight oxygen ions at the corners of two distorted tetrahedra. The (WO_4^{-2}) anions and the (Ca^{+2}) cations are ionically bonded in the overall tetragonal crystal structure. The site symmetry of both the calcium- and tungsten ions is S_4.

The symmetry of tungsten trioxide (WO_3) was given by Wyckoff[70] as monoclinic, pseudocubic, with a tetramolecular unit cell for which

$a = 7.274\,\text{Å}$; $b = 7.501\,\text{Å}$; $c = 3.824\,\text{Å}$; $\beta = 89°54'$

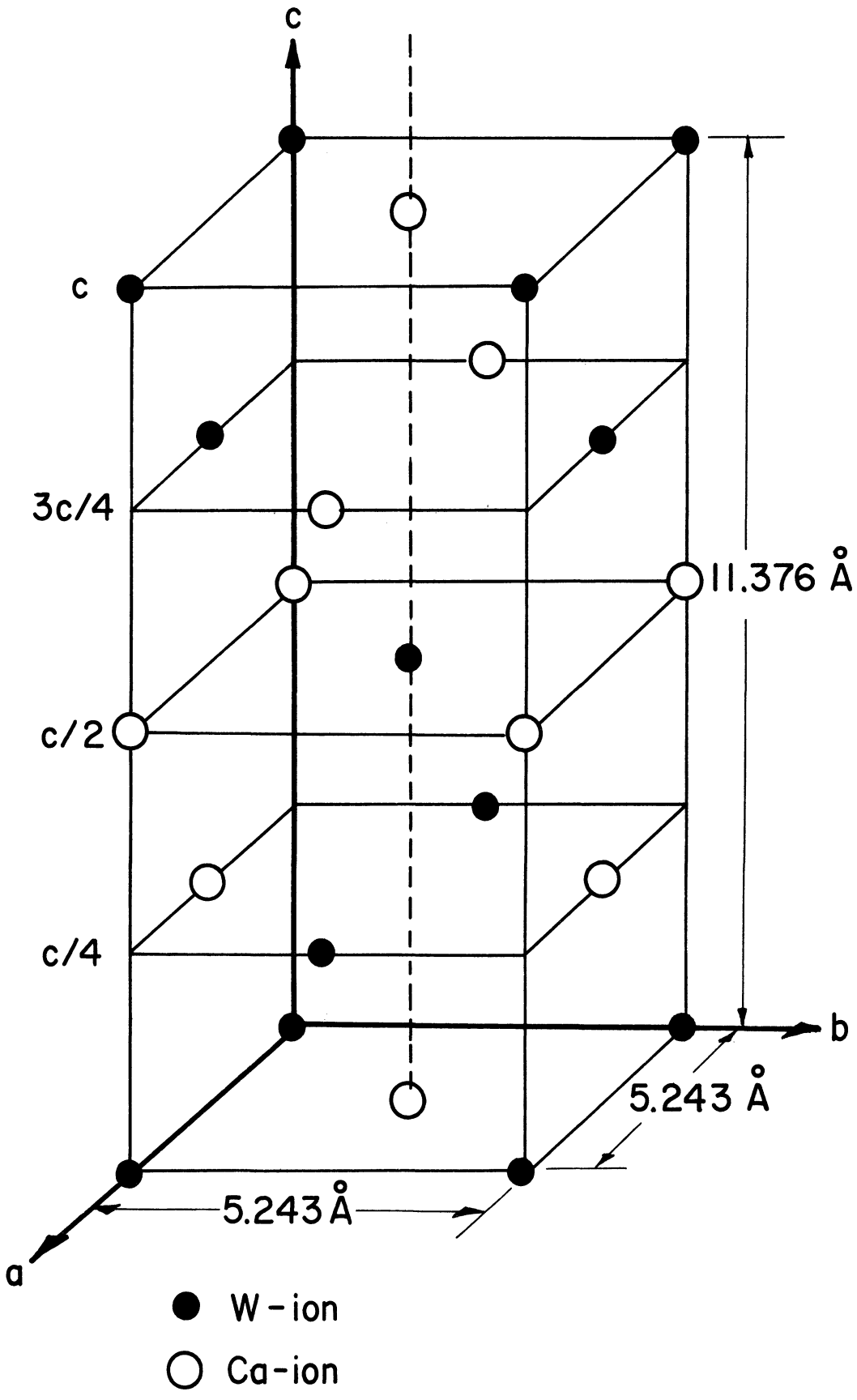

Figure 17

Metal Ions in $CaWO_4$ Unit Cell

The space group has been given as C_{2h}^5 or monoclinic $P2_1/a$ with all atoms in the general positions:

$$\pm(xyz;\ x+\tfrac{1}{2},\ \tfrac{1}{2}-y,\ z)$$

The atoms have the parameters:

	x	y	z
W	0.256	0.229	0.053
O(1)	0.250	0.030	0.000
O(2)	0.000	0.250	0.000
O(3)	0.250	0.280	0.500

This places six oxygen atoms around each tungsten atom at distances between 1.51 and 2.11 Å.

The positions of the three closest oxygen atoms to a tungsten site with the tunsten atom at the origin was calculated for a WO_3 complex by assuming orthorhombic symmetry ($\xi = 90°$). The WO_3 complex was then compared with a (WO_4^{-2}) radical to investigate the dimensional compatability of both complexes. This is shown in Figure 18. The dimensions of the (WO_4^{-2}) tetrahedron were taken from Chu[67]. The shaded area in (a) indicates the W-O bond lengths and the apex angles of one of the four possible positions within the (WO_4^{-2}) complex which can be occupied by the orthohombic WO_3. The orientation of the WO_3 complex in the (WO_4^{-2}) indicated by the shaded area in (b), was chosen such that the single W-O bond c of WO_3 coincides with the W-O(2) bond of (WO_4^{-2}) having the same length. Furthermore, approximately the same values were obtained for the W-O bond length a and the apex angle γ of WO_3 and (WO_4^{-2}). The close correspondence of two oxygen bonds, a and c, and one apex angle γ provides support for the possible substitution of WO_3 for (WO_4^{-2}).

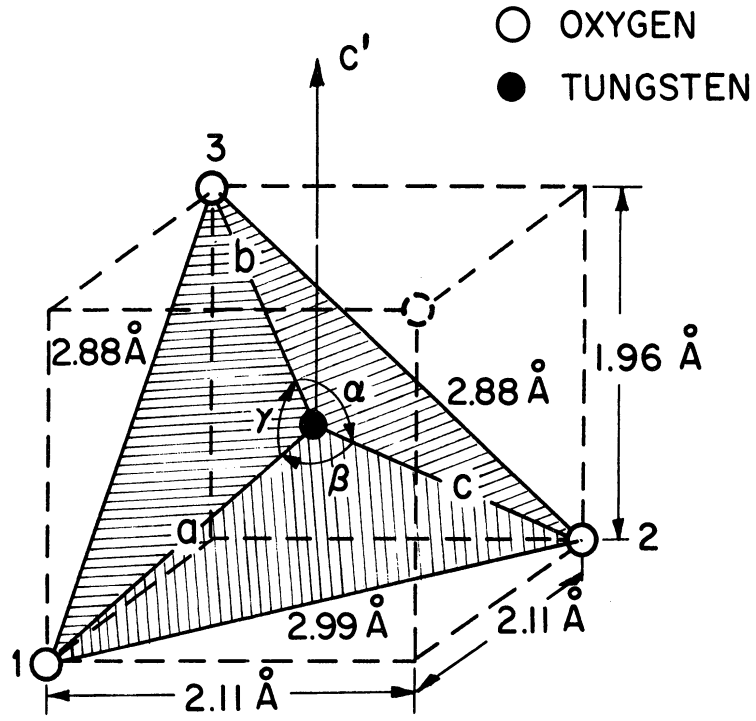

(a) (WO_4^{-2}) TETRAHEDRON

COMPLEX	a(Å)	b(Å)	c(Å)	α(°)	β(°)	γ(°)
WO_4^{-2}	1.78	1.78	1.78	70.7	65.4	70.7
WO_3	1.75	1.51	1.79	94.9	96.4	69.7

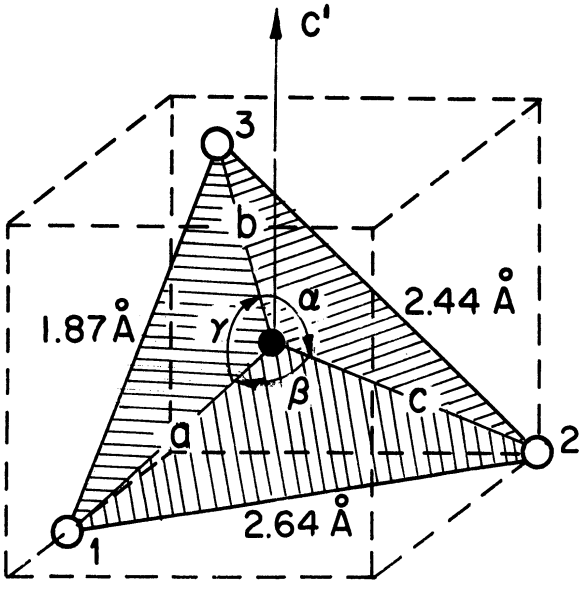

(b) WO_3 REPLACING (WO_4^{-2}) TETRAHEDRON

Figure 18

Tungstate (WO_4^{-2}) and Tungsten Trioxide (WO_3) Complexes

The formation of stoichiometric $CaWO_4$ is represented by the addition of calcium oxide (CaO) to tungsten trioxide (WO_3). However, in practice it is necessary to add an excess WO_3 to the melt[33] since WO_3 is highly volatile and will escape from the melt during crystal growth. Gmelin[68] states that excess WO_3 is readily soluble in $CaWO_4$ in small amounts (0.00012% at 1000°C) and permits satisfactory crystal growth despite the resulting nonstoichiometry in the melt. This excess WO_3 in the melt makes the presence of tungsten trioxide in $CaWO_4$ crystals highly probable. Furthermore, Nassau and Loiacono[33] reported that WO_3 in the solidified melt causes a green coloration of the $CaWO_4$ crystal. Such a coloration seemed to be present in the crystals used in this investigation*.

5.2 Fourth TL Peak - (Nb^{+4}) Ion

The trapped electrons responsible for the fourth TL peak in $CaWO_4$ are assigned to niobium of a NbO_4^{-4} complex in the tungsten site.

The correlation of TL and ESR results of gamma-irradiated $CaWO_4$ presented in section 3.3, indicated that the paramagnetic niobium (Nb^{+4}) spectrum can be identified with the fourth TL peak occurring at approximately 290°K. The experimentally determined g-values with the magnetic field in the (001) and (110) direction were given in section 3.3 and compared with the values reported by Chu[67]. The similarity of these g-values and the hyperfine separations provided convincing evidence that the same niobium (Nb^{+4}) center was observed. This niobium center

---

* Private communication with R.T. Farrar of the Harry Diamond Laboratories: approximately 1% WO_3 added to the melt

was assigned by Chu to a covalent tungsten site.

The assignment of Nb^{+4} to a covalent tungsten site rather than an ionic calcium site* was based in part on the following arguments[67]:

1. The niobium Nb^{+5} radius (0.70Å) is much closer to the tungsten W^{+6} radius (0.62Å) than the calcium Ca^{+2} radius (0.99Å).

2. The +5 valency of niobium is more likely to substitute for the +6 valency of tungsten than the +2 valency of calcium.

3. The substitution of niobium for tungsten has been inferred from chemical evidence.

4. Further evidence for niobium in the covalent tungsten site was obtained from the comparison of published ESR data on niobium and vanadium with the corresponding values of niobium obtained in this investigation. These results are shown below.

Sample	Δg_{001}**	A(gauss)	reference
zircon:Nb	-0.151	309	72
rutile:Nb	-0.035	90	65
Scheelite:			
$CaWO_4$:Nb	+0.0187	29	present work
$CaWO_4$:V	+0.0222	19.7	35

* The symmetry of the Nb^{+4} spectrum discussed in section 3.3 does not rule out the possibility of niobium in a calcium site, because both sites have the same point symmetry

** Deviation of g-value in the (001) direction from the free electron value of 2.0023

Large hyperfine separations (A) and negative Δg-values are reported for niobium in zircon and rutile. Chu[67] indicated that niobium is in a predominantly ionic site in both of these crystal structures. However, for niobium and vanadium in $CaWO_4$ small hyperfine separations and positive Δ g-values are obtained. Mahootian[35] assigned his group A vanadium spectrum to V^{+4} in a covalent tungsten site. The same arguments suggest that niobium in $CaWO_4$ is also in a covalent tungsten site* .

The roles of V^{+4} and Ta^{+4} on TL are discussed in section 4.1.

5.3 First TL Peak - $(W^{+5})_A$ Ion

It is proposed that the trapped electrons responsible for the 155°K TL peak are in a WO_4^{-3} complex which in turn is associated with nearby WO_3 and NbO_4^{-3} radicals.

Some of the electron spin resonance properties of $(W^{+5})_A$ are discussed in section 3.3. There, it was indicated that the Δg is positive. For example Δg_{001}=+0.0067. Hence applying the same arguments as used for Nb^{+4}, it is inferred that $(W^{+5})_A$ is in a predominantly covalent tungsten site such as WO_4^{-3}.

The direction of the largest principal axis (g_z) of the $(W^{+5})_A$ g-tensor suggests that the WO_4^{-3} complex is associated with a nearby oxygen ion. This axis (g_z) is approximately along the direction of the second nearest oxygen. Figure 19 shows this oxygen (4) and g_z. The

---

* For further comments see Karavelas[73]

O-SITE	θ	ϕ	R
1	22°20'	59°41'	4.1336 Å
2	157°40'	329°41'	4.1336 Å
3	50° 2'	-55°25'	2.9023 Å
4	129°58'	34°35'	2.9023 Å
$g_z(W^{+5})_A$	116°14'	37°57'	

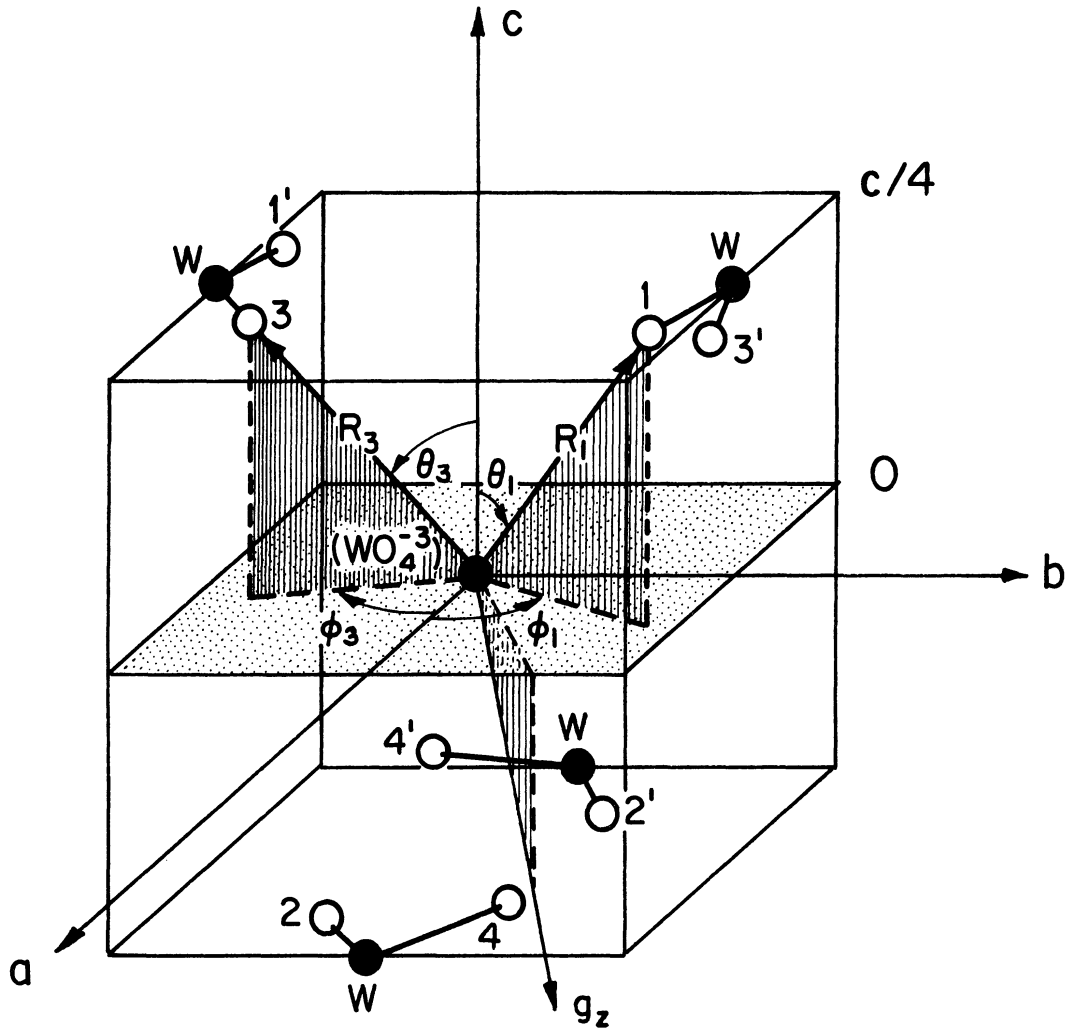

Figure 19

Positions of Second Nearest Oxygen Ions to Tungsten Ion of (WO_4^{-3}) Complex. Prime Superscripts Refer to $(\pi+\phi)$. O- Oxygen Ions.

corresponding angles are:

	Θ	ϕ
Oxygen (4)	129° 58'	34° 35'
g_z $(W^{+5})_A$	116° 14'	37° 57'

It is proposed that this principal axis is in the direction of the oxygen vacancy associated with the WO_3 complex. As shown in Figure 18, the substitution of WO_3 for WO_4^{-2} is possible in view of the similarities in oxygen positions.

Finally, evidence for associating the WO_4^{-3} complex with a nearby NbO_4^{-3} is suggested by the observations that the fourth TL peak intensity and the Nb^{+4} lines increased upon thermal annealing of the first TL peak and the $(W^{+5})_A$ spectrum respectively. These observations were made only at low irradiation dosages.

Figure 20 presents a model of the lattice defect which can account for the observed results for $(W^{+5})_A$. Indicated is the WO_4^{-3} complex with the largest principal axis of the $(W^{+5})_A$ g-tensor in the direction of an oxygen vacancy associated with a nearby WO_3 complex. This WO_3 is thought to be associated with a calcium (Ca^{+2}) ion which provides the two extra positive charges for two neighboring $CaNbO_4^{-1}$ complexes.

The absence of the first TL peak for all trivalent rare earth ion (RE^{+3}) doped $CaWO_4$ crystals (Figure 18) can be explained by the proposed lattice defect model. Suppose that two RE^{+3} ion occupy two of the Ca^{+2} sites next to the NbO_4^{-3} complexes. The remaining calcium ion associated with the two niobate radicals is now no longer needed and combines with the WO_3 complex and an extra oxygen to form a neutral $CaWO_4$ molecule. The consequence is that the RE^{+3} ion doping will remove

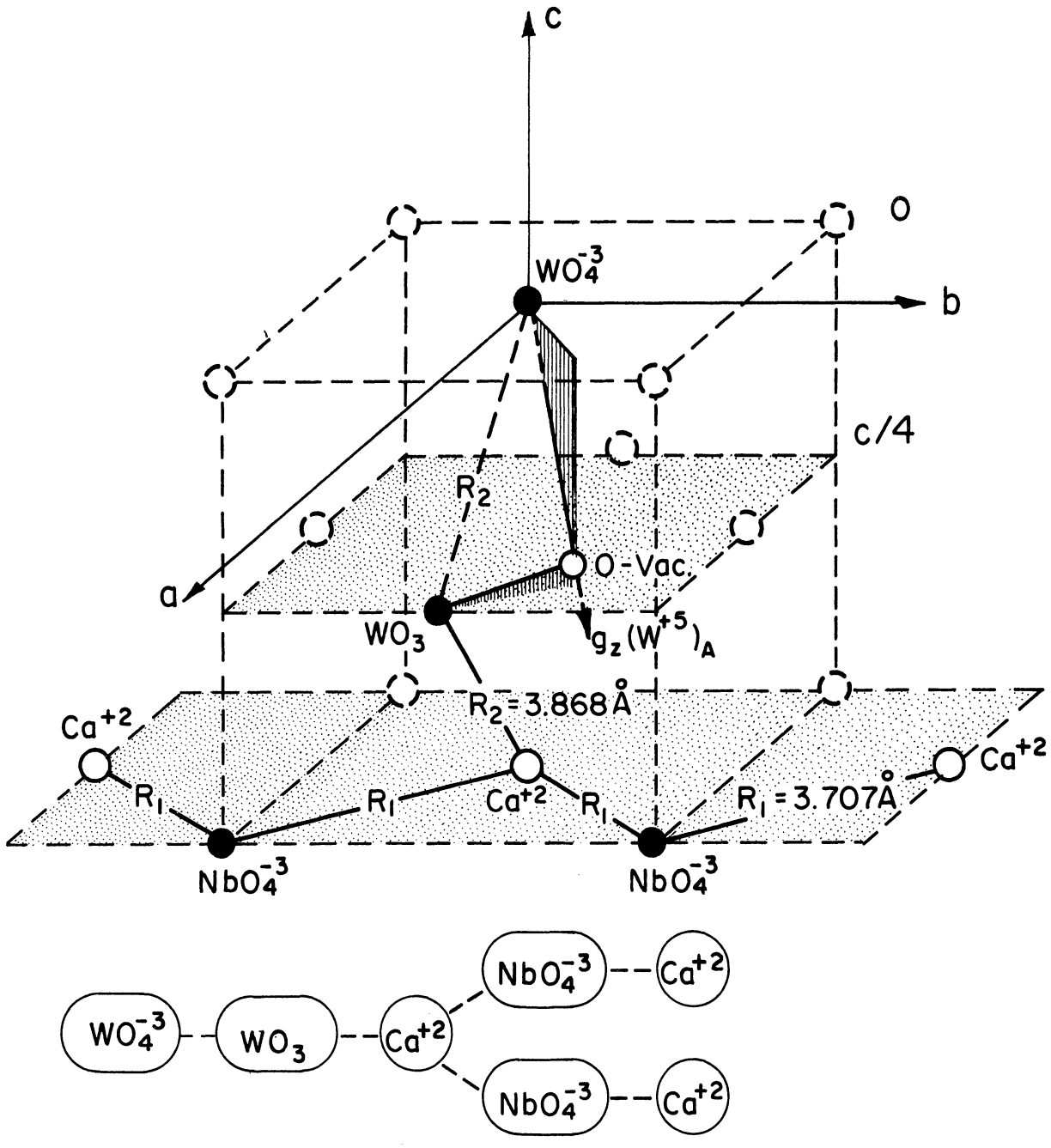

Figure 20

Lattice Defect Model Associated With Trapping Center in (WO_4^{-3}) Complex

these WO_3 complexes. This removal of WO_3 will eliminate the trapping centers in the WO_4^{-2}. It is expected that nearly all WO_3 complexes are removed in the 0.2% to 0.5% RE^{+3} doped $CaWO_4$ samples used in this investigation, since only 0.03% (atomic percent) unintended niobium Nb^{+4} was observed in the $CaWO_4$ crystals.

5.4 Second TL Peak - $(W^{+5})_B$ Ion

Arguments are presented for the proposed assignment of the trapped electrons responsible for the 225°K TL peak, to a WO_3^{-1} complex with a nearby calcium defect.

Electron spin resonance measurements showed (section 3.3) that the $(W^{+5})_B$ spectrum is associated with the second TL peak. The negative Δg_{001}-value (-0.1593) and the large hyperfince separation (60 gauss) implies that the $(W^{+5})_B$ ion is not in a covalent tungsten site of a WO_4^{-2} complex but bonded in a predominantly ionic tungsten site. Such an ionic site is assumed to exist in a neutral WO_3 complex.

Figure 21 illustrates the proposed model for the $(W^{+5})_B$ center. The WO_3 in the WO_4^{-2} site is indicated by the oxygen positions (1), (2), and (3). Using the same numbering of the oxygen positions as that adopted for the WO_3 complex in Figure 18, the W-O bonds a and c are W-O(1) and W-O(2) respectively; the angle γ is O(3)-W-O(1). The corresponding values are the following:

	a(A°) W-O(1)	c(A°) W-O(2)	γ(°) O(3)-W-O(1)
WO_4^{-2}	1.78	1.78	70.7
WO_3	1.75	1.79	69.7

SITE	θ	ϕ	R
OXYGEN 1	56°44'	31°54'	1.78 Å
CALCIUM 4	90°	45°	3.71 Å
$g_y(W^{+5})_B$	96°24'	33°11'	
OXYGEN 3	123°16'	-58°6'	1.78 Å
$g_x(W^{+5})_B$	89°31'	-55°36'	

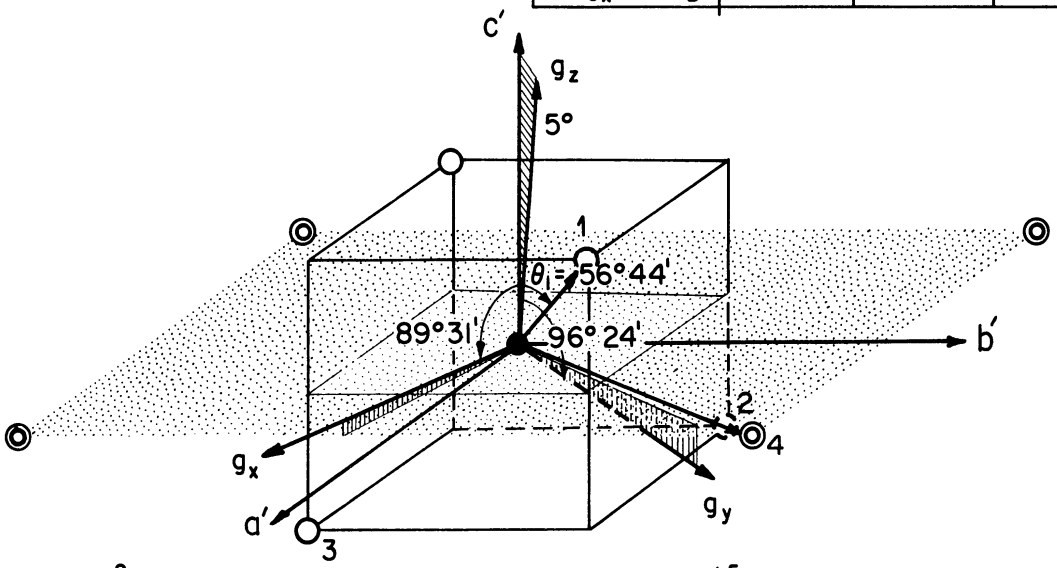

(a) (WO_4^{-2}) TETRAHEDRON, PRINCIPAL AXES OF $(W^{+5})_B$ TENSOR, AND CALCIUM ATOMS IN a'b'-PLANE

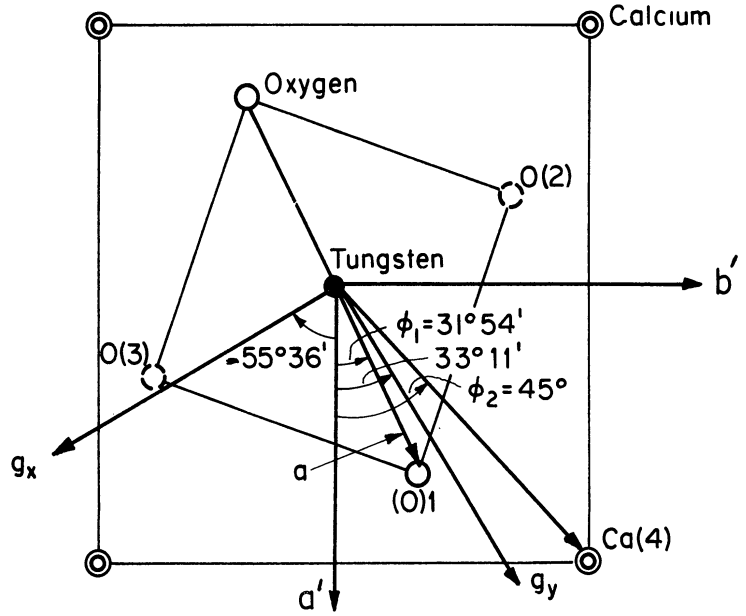

(b) PROJECTION OF (WO_4^{-2}) TETRAHEDRON AND PRINCIPAL AXES (g_x, g_y) OF $(W^{+5})_B$ TENSOR ON CALCIUM PLANE (a'b'- PLANE)

Figure 21

Comparison of Principal Axes of $(W^{+5})_B$ g-Tensor With Nearest Oxygen and Calcium Positions to Tungsten Site

The similarity of the angles ϕ for the projection of the principal axis (g_y) of the $(W^{+5})_B$ g-tensor and the oxygen bond (W-O(1)) onto the a'b'-plane with the direction of the calcium position (W-Ca(4)) suggests that the WO_3^{-1} complex is associated with a nearby calcium defect. The values of the angles ϕ are as follows:

	O(1)	Ca(4)	$g_y(W^{+5})_B$
ϕ	31°54'	45°	33°11'

Corresponding similarities were observed for the principal axis (g_x), one oxygen bond (W-O(3)), and one calcium position.

A comparison of the ESR results reported by Azarbayejani[69] for paramagnetic tungsten W^{+5} in vacuum reduced $CaWO_4$:Y with those of the $(W^{+5})_B$ center suggested that the same paramagnetic center was observed. These ESR results are shown below:

	Sample	ion	g_{001}	g_{110}	A(gauss)
Azarbayejani	$CaWO_4$:Y	W^{+5}	1.850	1.593	19-66
Present work	$CaWO_4$	$(W^{+5})_B$	1.843	1.605	35-65

It is probable that Azarbayejani's center is associated with an oxygen defect. Because of the high oxygen mobility*, the oxygen defects may migrate through the crystal and associate with calcium vacancies. Such an oxygen-calcium vacancy could be interpreted as a WO_3 complex with a calcium deficiency which was assigned to the $(W^{+5})_B$ ion.

---

* Reoxidation of reduced $CaWO_4$ takes place at 1000°C in an oxygen atmosphere in a few minutes[33], demonstrating the ready mobility of oxygen in $CaWO_4$.

It seems appropriate at this point to mention briefly the two paramagnetic tungsten W^{+5} centers reported by Chu in fast neutron irradiated $CaWO_4$. One center $(W^{+5})_\gamma$ was associated with a nearest oxygen deficiency (gamma center)[63] and the other $(W^{+5})_\beta$ with a nearest calcium displaced (beta center)[67]. The ESR results of these centers are listed below together with those of the $(W^{+5})_B$ center.

	Ion	g_{001}	g_{110}	A(gauss)
Chu	$(W^{+5})_\beta$	1.810	1.757	51-120
Chu	$(W^{+5})_\gamma$	1.745	1.710	280-320
Present Work	$(W^{+5})_B$	1.843	1.605	35-65

A comparison of the g-values and the hyperfine constants (A) indicates that the fast neutron produced paramagnetic tungsten centers of Chu are not the same as the $(W^{+5})_B$ center. This is not unexpected since the removal of oxygen and calcium ions by fast neutron bombardment may create other local disturbances which prevent the vacancies from migrating through the crystal as was postulated for Azarbayejani's tungsten center. This argument is supported by the low annealing rate of Chu's centers at 300°K as compared to the complete removal of the $(W^{+5})_B$ center at 250°K.

V CONCLUSION

The investigation of trapping centers in pure $CaWO_4$ presented in this thesis, shows that identification of trapping sites is possible by correlating TL and ESR measurements.

Three major trapping centers were found in the tungsten sites of gamma-irradiated pure $CaWO_4$. Two of those occurring at low temperatures (shallow traps) are associated with lattice defects whereas the high temperature electron trap (deep trap) is attributed to unintended impurities. The results which led to the identification of the three trapping centers in $CaWO_4$ are summarized in the three rows of Table III.

A possible model for the trapping center responsible for the first major TL peak of pure $CaWO_4$ is a paramagnetic tungsten (W^{+5}) ion in a (WO_4^{-3}) associated with a nearby WO_3 and NbO_4^{-3} complex. The trap depth corresponding to this 155°K TL peak is aobut 0.36 ev. The g-value is 2.009 when the magnetic field is along the c-axis.

The second TL peak occurring at approximately 225°K, is identified with a different paramagnetic tungsten (W^{+5}) ion and tentatively assigned to a (WO_3^{-1}) complex with a neighboring calcium deficiency. The trap depth is about 0.55 ev and $g_{001}=1.843$.

A paramagnetic niobium (Nb^{+4}) ion in a tungsten site and assigned to a (NbO_4^{-4}) complex is responsible for the fourth major TL peak. The trap depth is 0.72 ev and the numerical value of g_{001} is 2.021.

The method used in this investigation for the identification of trapping centers in $CaWO_4$ seems to be applicable to similar investigations of electron traps in semiconductor and insulator materials.

TABLE III

TL AND ESR RESULTS OF GAMMA-IRRADIATED NOMINALLY PURE $CaWO_4$

ORDER OF TL PEAK	EFFECTIVE TL PEAK TEMP. (°K)	TRAP ENERGY (ev)	PARAMAGNETIC ION ASSOCIATED WITH TL PEAK	SITE OF PARAMAGNETIC ION	COMPLEX(ES) ASSOCIATED WITH PARAMAGNETIC ION
1	155±10	0.36±.02	W^{+5} $g_{001} = 2.009$	TUNGSTEN	WO_4^{-3} with nearby WO_3 and NbO_4^{-3}
2	225±10	0.55±.02	W^{+5} $g_{001} = 1.843$	TUNGSTEN	WO_3^{-1} with calcium vacancy
4	290±10	0.72±.02	Nb^{+4} $g_{001} = 2.021$	TUNGSTEN	NbO_4^{-4}

APPENDIX I

Randall-Wilkins' Equation[46]

The Randall-Wilkins equation (8) was used to find a relationship between the trap depth and the frequency factor from the experimental TL curves for each TL peak of pure $CaWO_4$. This equation is based on the assumption that the trapped electrons have a Maxwellian distribution of thermal energies; hence the probability P(E,T) of an electron escaping from a trap of depth E (thermal or optical activation energy) at temperature T is of the form

$$P(E,T) = s \exp\left(-E/kT\right) \tag{1}$$

Where k is the Boltzmann constant and s the frequency factor, describing the frequency of electron movement in the traps. The ionization rate is proportional to this escape probability. Equation (1) assumed no temperature dependence of the frequency factor s.

The rate of change of the number of electrons in the traps is expressed by:

$$\left(dn/dt\right) = n P \tag{2}$$

where n is the number of filled traps at time t (number of trapped electrons). The retrapping of the electrons is neglected in equation(2).

Combining equations (1) and (2) yields:

$$I = -\left(dn/dt\right) = ns \exp\left(-E/kT\right) \tag{3}$$

Solving equation (3) for n results in:

$$n = n_0 \exp\left[-\frac{s}{\beta}\int_{T_i}^{T} \exp\left(-E/kT'\right) dT'\right] \tag{4}$$

where

$$\beta = \left(dT/dt\right) \tag{5}$$

Here, I denotes the luminescent intensity, n_0 the number of trapped electrons at time t=0 (area below the TL curve and above the thermal background curve), and β the heating rate. The TL intensity is now obtained from equations (3) and (4).

$$I = n_0 s \exp\left(-E/kT\right) \exp\left(-\frac{s}{\beta}\int_{T_i}^{T} \exp\left[-E/kT'\right] dT'\right) \tag{6}$$

Integration by parts of equation (6) results in:

$$\frac{I}{n_0} = s \exp\left(-E/kT\right) \exp\left[-\frac{s}{\beta}\left(T\frac{\exp\left[-E/kT\right]}{E/kT} - T_i\frac{\exp\left[-E/kT_i\right]}{E/kT_i}\right)\right] \tag{7}$$

where

$$\int_{T_i}^{T} \exp\left(-E/kT'\right) dT' \simeq T\frac{\exp\left[-E/kT\right]}{E/kT} - T_i\frac{\exp\left[-E/kT_i\right]}{E/kT_i}$$

Equation (7) was used to calculate a curve of (I/n_0) versus T which was then matched with the experimental TL peak by varying the trap depth E and frequency factor s. This procedure made use of the TL peak intensity I_{max}, peak temperature T_{max}, starting temperature T_i, and heating rate β .

Since at the peak intensity

$$\left(dI/dT\right)_{max} = 0$$

using equation (6), this gives:

$$s = \left(\beta/T_{max}\right)\left(E/kT_{max}\right)\exp\left(E/kT_{max}\right) \tag{8}$$

Equation (8) represents nearly a straight line of log(s) versus E, since $(E/kT_{max}) \gg 1$; i.e. $E/kT_{max} > 20$ for the peak temperatures and trap depths of TL. This equation makes use only of the TL peak

temperature T_{max} and heating rate β .

Combining equations (3) and (7) yields:

$$(9) \quad n = n_0 \exp\left[-\frac{s}{\beta}\left(T\frac{\exp\left[-E/kT\right]}{E/kT} - T_i\frac{\exp\left[-E/kT_i\right]}{E/kT_i}\right)\right]$$

Equation (9) evaluated at the TL peak temperature T_{max} results in:

$$(10) \quad n^* = n_0 \exp\left[-\frac{s}{\beta}\left(T_{max}\frac{\exp\left[-E/kT_{max}\right]}{E/kT_{max}} - T_i\frac{\exp\left[-E/kT_i\right]}{E/kT_i}\right)\right]$$

where n* represents the number of electrons left in the traps at T_{max}. Substituting equation (8)

$$(8) \quad \frac{\exp\left[-E/kT_{max}\right]}{E/kT_{max}} = \frac{\beta}{sT_{max}}$$

into equation (10), yields an expression for n*

$$(11) \quad n^* = n_0 \exp\left[-1\right] \exp\left[\frac{s}{\beta}T_i\frac{\exp\left[-E/kT_i\right]}{E/kT_i}\right]$$

Since $E/kT_i \gg 1$ for the TL starting temperatures and trap depths of interest, equation (11) may be written as:

$$(12) \quad \boxed{n^* \simeq n_0 \exp\left[-1\right]}$$

Equation (12) indicates that approximately 1/e of the original number of electrons remain in the traps upon heating to the TL peak temperature T_{max}.

APPENDIX II

Vasileff's Expression[56]

The theory of the thermal ionization of a trapped electron in an ionic crystal, which was developed by Vasileff, provided an expression relating the frequency factor to the trap depth. This expression, given by equation (15), was used to calculate the trap depth in terms of the energy and temperature dependent frequency factor for the three major TL peaks of pure $CaWO_4$. The constants needed for the calculation and a sample calculation are also given.

Vasileff associated the thermal ionization of an electron, trapped at an interstitial lattice site, with a multiple phonon absorption process, because the lattice vibrations are responsible for the energy transfer between the lattice and the trapped electron. This defines the trap energy E.

(13) $E = q_i \hbar \omega_\ell$ $\quad q_i = p$ positive integer

$q_i = y$ positive non-integer

where p is the smallest integer greater than y. In equation (13), p represents the number of absorbed phonons and ω_ℓ the longitudinal optical phonon frequency.

The rate of thermal ionization of the electron was found from the transition probability between the ground state of the trapped electron and the conduction band, summed over all states of the conduction band. For this calculation, Vasileff assumed a hydrogenic wave function for the ground state (electron in trap) and a plane wave function for the electron in the conduction band. Harmonic oscillator wave functions were assumed for the lattice vibration. The resulting expression given by Vasileff for the ionization rate was:

$$(14)\quad P(E,T_{eff}) = \frac{A S^{p-1} z^{1/2}}{2^{p-1}\,\Gamma(p)} \left(\exp[\gamma]-1\right) \exp\left(\frac{\gamma}{2}\right) \exp\left(-S\coth\left[\frac{\gamma}{2}\right]\right) \exp\left[-\frac{p\gamma}{2}\right]\left[\sinh\left(\frac{\gamma}{2}\right)\right]^{1-p}$$

where

$$A = 9\pi^{1/2}\left(\frac{3}{4\pi}\right)^{1/3} 2^{17}\,\omega_t^{3/2}\, m^{*7/2}\,(ee^*)^2 \frac{V}{h^{9/2}\,M}\left(\frac{\varepsilon_0}{\varepsilon_\infty}\right)^{3/4}\left(\frac{\varepsilon a_0^*}{V^{1/3}}\right)^7 F_3(\xi)$$

$$\xi = 2\pi\left(\frac{3}{4\pi}\right)^{1/3} V^{-1/3}$$

$$F_3(\xi) = \frac{1}{10}\left(1+\eta^2\right)^{-5} - \frac{11}{80}\left(1+\eta^2\right)^{-4} + \frac{1}{160}\left(1+\eta^2\right)^{-3} + \frac{1}{128}\left(1+\eta^2\right)^{-2} + \frac{3}{256}\left(1+\eta^2\right)^{-1} + \frac{3}{256}\eta^{-1}\tan^{-1}(\eta)$$

$$\eta = \alpha\xi$$

$$\alpha = \varepsilon\hbar^2\left(2m^* e^2\right)^{-1}$$

$$S = 16\pi^2\left(\frac{3}{4\pi}\right)^{1/3}(ee^*)^2\left(\hbar\omega_t^3\, M V^{4/3}\right)^{-1}\left(\frac{\varepsilon_\infty}{\varepsilon_0}\right)^{3/2} F_1(\xi)$$

$$F_1(\xi) = \frac{1}{6}\left(1+\eta^2\right)^{-3} + \frac{5}{24}\left(1+\eta^2\right)^{-2} + \frac{5}{16}\left(1+\eta^2\right)^{-1} + \frac{5}{16}\eta^{-1}\tan^{-1}(\eta)$$

$$\gamma = \hbar\omega_e/kT_{eff} \qquad z = p - y$$

$$\frac{1}{\varepsilon} = \frac{1}{16}\left(\frac{5}{\varepsilon_\infty} + \frac{11}{\varepsilon_0}\right) \qquad a_0^* = \hbar^2/m^* e^2$$

$$\omega_e^2 = \omega_t^2\left(\frac{\varepsilon_0}{\varepsilon_\infty}\right)$$

The energy and temperature dependent frequency factor $s(E,T_{eff})$ is now expressed by equation (15):

$$(15)\quad \boxed{s(E,T_{eff}) = P(E,T_{eff})\exp(p\gamma)}$$

This equation was used for finding a relationship between the trap depth E and the frequency factor $s(E,T_{eff})$.

The constants needed to obtain numerical values for this relationship between the trap depth and the frequency factor of pure $CaWO_4$, have been summarized below.

m^* = 9.108×10^{-28} gm ..... effective mass of electron in conduction band

ω_t = 4.6×10^{13} c/sec ($240\ cm^{-1}$) ..... transverse optical phonon frequency (Reststrahl frequency) (Ref. 27)

ε_o = 8.0 @ 10 Mc/sec ..... static dielectric constant (Ref.25)

ε_∞ = 3.6 ..... High-frequency dielectric constant (Ref. 26)

M = 5.74×10^{-23} gm ..... reduced mass of $CaWO_4$ diatomic model

V = 7.81×10^{-23} cm^3 ..... volume of $CaWO_4$ diatomic model (volume of unit cell = $3.125 \times 10^{-22} cm^3$)

e^* = $2 \times 4.8 \times 10^{-10}$ esu ..... effective charge of ions in diatomic molecule

a = 5.25×10^{-8} cm ..... lattice parameter (Ref. 62)

c = 11.37×10^{-8} cm ..... lattice parameter (Ref. 62)

k = 1.38×10^{-16} erg $^\circ K^{-1}$ .... Boltzmann's constant

$\hbar$ = 1.05×10^{-27} erg sec..... Dirac's constant

e = 4.8×10^{-10} esu ..... charge of electron

Using the above constants in the preceeding equations, the following quantities are:

A = 1.08×10^{13} sec^{-1}

ξ = 9.12×10^{7} cm^{-1}

$F_3(\xi)$ = 1.17×10^{-2}

η = 1.40

α = 1.53×10^{-8} cm

S = 17.74

$F_1(\xi)$ = 0.35

z = 0.24

ε = 5.79

a^*_o = 5.29×10^{-9} erg/cm^2/esu^2

ω_e = 6.86×10^{13} c/sec

The values calculated from equations (14) and (15) for the first TL peak of pure $CaWO_4$ at an effective TL peak temperature T_{eff}=155°K and trap depth E=0.35 ev, are:

$$P(E,T_{eff})=7.92\times10^{-3}\ sec^{-1}$$

$$s(E,T_{eff})=4.36\times10^{9}\ sec^{-1}$$

APPENDIX III

Summary of Commonly Use Methods for Finding the Trap Depth and Frequency Factor

Several methods have been used in the past for finding values of the trap depth from the experimental TL curves. These methods or equations are summarized in this section since they were applied to the three major TL peaks of nominally pure $CaWO_4$.

Equation (8) of Appendix I

$$E = \kappa T_{max}^2 s \beta^{-1} \exp\left[-E/\kappa T_{max}\right] \tag{8}$$

showed that a trap depth value may be calculated only after assuming a frequency factor. However, the frequency factor in equation (8) may be eliminated by using two heating rates and the corresponding peak temperatures for the same TL peak. Hence, the trap depth may be found from:

$$E = \frac{\kappa}{T_{max}^{-1})_2 - T_{max}^{-1})_1} \ln\left(\frac{\beta_1 T_{max}^2)_2}{\beta_2 T_{max}^2)_1}\right) \tag{16}$$

where $\beta_1 > \beta_2$ implies $T_{max})_1 > T_{max})_2$. Equation (8) may be used to find the corresponding frequency factor s.

Grossweiner[48] used equation (6) of Appendix I and a point on the low temperature side of the TL peak (I_1, T_1) at which the luminescent intensity is $T_{max}/2$, for evaluating the trap depth E.

$$E = 1.51\, \kappa \frac{T_1 T_{max}}{T_{max} - T_1} \tag{17}$$

and the corresponding frequency factor s

$$(18)\quad s = \frac{3\beta T_1 \exp\left[E/k_B T_{max}\right]}{2T_{max}\left[T_{max} - T_1\right]}$$

A discussion of this procedure is also given in reference 58.

Using equation (8) of Appendix I and plotting trap depth versus peak temperature for various heating rates and frequency factors resulted in straight lines of the form

$$(19)\quad \boxed{E = T_{max}/A}$$

Urbach[49] obtained satisfactory results for the trap depth E in ev for ZnS(Cu) by using

$$A = 500 \text{ for } \quad \beta = 1^\circ K/sec$$

$$A = 400 \text{ for } \quad \beta = 0.01^\circ K/sec$$

The frequency factor was evaluated from equation (11).

Two points on the rising part of each TL peak - (I_1, T_1) and (I_2, T_2) - were used by Katz[50] for finding the trap depth E:

$$(20)\quad \boxed{E = k_2 \frac{T_1 T_2}{T_2 - T_1} \ln\left(\frac{I_2}{I_1}\right)}$$

Using the half-width at one-half-maximum (δ_m) of each TL peak, Rabkin and Konevskaya[51] employed the following expressions for evaluating the trap depth E and frequency factor s.

$$(21)\quad \boxed{E = k_2 T_{max}^2 \delta_m^{-1}}$$

$$s = \beta \delta_m^{-1} \exp\left[T_{max}/\delta_m\right]$$

Equation (3) of Appendix I indicates that the initial rise of a TL peak is governed by the exponential:

$$(22)\quad \boxed{I \propto \exp\left[-E/k_2 T\right]}$$

The value for the trap depth E can be found from the slope of the straight line of ln(I) versus T^{-1}, constructed from the experimental TL curve. However, additional minor peaks are usually observed with the major TL peaks. The removal of these additional peaks from the rising part of the major peaks resulted in constant values of the slope or trap depth.

This method for finding a trap depth value can be applied also to the high temperature side of a TL peak, if the peaks are well separated.

A method which uses the total experimental TL intensity trace of I(t) versus t directly for finding the trap depth E and the frequency factor s, was described by Bucci, Fieschi, and Guidi[52], and Scaramelli[53]. This method is given by equation (23):

(23) $$\boxed{\ln(s) = \frac{E}{k} T^{-1} - \ln\left(A_t / I(t)\right)}$$

where $$A_t = \int_{t_0}^{t} I(t')\,dt'$$

Thus, finding the partial areas underneath the TL peak (A_t) and dividing by the respective ordinate (I_t), results in a straight line of ln(s) versus 1/T. The slope of the line corresponding to the rising part of the TL peak represents the trap depth E. The intercept results in the corresponding frequency factor s.

REFERENCES

1. A. J. Oszy, "The Excitation Spectra of Some Tungstate", J. Opt. Soc. Am., 41, 57 (1951)

2. F. A. Kroeger, "Some Aspects of the Luminescence of Solids", Elsevier Publ. Co., 107-221 (1948)

3. R. H. Gillette, "Calcium and Cadmium Tungstate as Scintillation Counter Crystals for Gamma-Ray Detection", Rev. Sc. Instr., 21, 294 (1950)

4. G. B. Beard, W. H. Kelly, M. L. Mallory, "Temperature Dependent Luminescence of $CaWO_4$ and $CdWO_4$", J. Appl. Phys., 33, 144 (1962)

5. M. Sayer, W. R. Hardy, "Scintillation Decay in Calcium Tungstate", Can. J. Phys., 43, 1925 (1965)

6. W. R. Dawson, J. L. Kropp, M. W. Windsor, "Internal-Energy-Transfer Efficiency in Eu^{3+} and Tb^{3+} Chelates Using Excitation to Selected Ion Levels", J. Chem. Phys., 45, 2410 (1966)

7. G. H. Dieke, B. Pandey, "Absorption, Fluorescence, and Energy Levels of Ho^{3+} in Hexagonal $LaCl_3$", J. Chem. Phys., 41, 1952 (1964)

8. G. H. Dieke, H. M. Crosswhite, "The Spectra of the Doubly and Triply Ionized Rare-Earths", Appl. Opt., 2, 675 (1963)

9. G. S. Ofelt, "Structure of the f^6 Configuration with Application to Rare-Earth Ions", J. Chem. Phys., 38, 2171 (1963)

10. G. H. Dieke, R. Sarup, "Fluorescence Spectrum and the Energy Levels of the Sm^{2+} Ion", J. Chem. Phys., 36, 371 (1962)

11. L. G. Van Uitert, R. R. Soden, "Emission Spectra of Trivalent Terbium", J. Chem. Phys., 32, 1161 (1960)

12. K. S. Thomas, S. Singh, G. H. Dieke, "Energy Levels of Tb^{3+} in $LaCl_3$ and Other Chlorides", J. Chem. Phys., 38, 2180 (1963)

13. L. G. Van Uitert, L. F. Johnson, "Energy Transfer between Rare-Earth Ions", J. Chem. Phys., 44, 3514 (1966)

14. H. A. Koehler, C. Barnes, C. Kikuchi, "Double-Photon Absorption in $CaWO_4$:1% Nd^{3+}", Bull., Am., Phys., 10, 608 (1965)

15. W. Viehmann, "Influence of Charge Compensation on UV Excitation of Rare-Earth Fluorescence", J. Chem. Phys., 47, 875 (1967)

16. L. F. Johnson, "Characteristic of the $CaWO_4:Nd^{3+}$ Optical Maser", Quant . Electr., 2, Paris (1963)

17. K. C. Chu, C. Kikuchi, W. Viehmann, "ESR of Niobium in $CaWO_4$", J. Chem. Phys., 46, 386 (1967)

18. P. A. Forrester, D. F. Hempstead, "Paramagnetic Resonance of Tb^{3+} Ions in $CaWO_4$ and CaF_2", Phys. Rev., 126, 923 (1962)

19. R. W. Kedzie, M. Kestigian, "PMR Determination of Transition Metal Ion Sites and Multiplicity of Rare-Earth Ion Sites in $CaWO_4$", Appl. Phys. Lett., 3, 86 (1963)

20. R. W. Kedzie, M. Kestigian, "PMR of Nd^{3+} in $CaWO_4$", Appl. Phys. Lett., 4, 124 (1964)

21. C. G. B. Garrett, F.R. Merritt, "PMR Spectra of Nd^{3+} in Compensated and Uncompensated $CaWO_4$", Appl. Phys. Lett., 4, 31 (1964)

22. T. U. Ranon, "Electron Spin Resonance of $CaWO_4$:Nd^{3+}", Phys. Lett., 8, 154 (1964)

23. J. Kirton, "PMR of Ho^{3+} Ions in $CaWO_4$", Phys. Rev., 139A, 1930 (1965)

24. I. Z. Potvorova, L. Ya. Shekun, "EPR Study of Tetragonal Sm^{3+} Centers in $CaWO_4$", Sov. Phys. Sol. State, 7, 2596 (1966)

25. K. Nassau, A. M. Broyer, "Calcium Tungstate: Czochralski Growth, Perfection, and Substitution", J. Appl. Phys., 33, 3064 (1962)

26. A. S. Barker, "Infrared Lattice Vibrations in Calcium Tungstate and Calcium Molybdate", Phys. Rev., 135, A742 (1964)

27. B. Cockayne, J. D. Ridley, "Scheelite Structures: Single Crystal Growth and Transmission Data", Nat., 203, 1054 (1964)

28. H. J. Levinstein, G. M. Loiacono, K. Nassau, "Calcium Tungstate II, Observation of Dislocations", J. Appl. Phys., 34, 3603 (1963)

29. J. P. Russell, R. Loudon, "The First-Order Raman Spectrum of $CaWO_4$", Proc. Phys. Soc., 85, 1029 (1965)

30. S. P. S. Porto, J. F. Scott, "Raman Spectra of $CaWO_4$, $SrWO_4$, $CaMoO_4$, and $SrMoO_4$", Phys. Rev., 157, 716 (1967)

31. C. Kikuchi, N. Mahootian, W. Viehmann, R. T. Farrar, "Vanadium Charge Compensator Site in Laser $CaWO_4$", Proc., 8th. Annual Electron and Laser Beam Symposium, University of Michigan (1966)

32. K. Nassau, "Substitution and Charge Compensation in CaWO4-Optical Maser Crystals", Quantum Electronics, I, Paris Conference (1963)

33. K. Nassau, G.M.L. Loiacono, "Calcium Tungstate-III, Trivalent Rare-Earth Substitution", J. Phys. Chem. Sol., 24, 1503 (1963)

34. K. Nassau, "Calcium Tungstate-IV, The Theory of Coupled Substitution", J. Phys. Chem. Sol., 24, 1511 (1963)

35. N. Mahootian, C. Kikuchi, W. Viehmann, "Spin Resonance Properties of Scheelites I. Vanadium in $CaWO_4$", J. Chem. Phys., 48, 1097 (1968)

36. J. R. Cook, "Trap Distribution of Calcium Tungstate Single Crystals", Proc. Phys. Soc., 71, 422 (1958)

37. V. L. Levshin, V. B. Guman, E.N. Karzhavina, "On the Possibility of Recombination Processes in the Luminescence of Tungstate and Uranyl Compounds", Opt. Spectra., VI, 234 (1959)

38. D. Hahn, K. Lertes, "Haftstellenerzeugung und Leuchtmechanismus bei den Wolframat-Phosphoren", Z. Phys., 169, 33 (1962)

39. P. Braunlich, K. Reibner, A. Scharmann, "Lumineszenz- und Leitfaehigkeitsuntersuchungen an $CaWO_4$-Einkristallen", Z. Phys., 183, 431 (1965)

40. M. Sayer, A. Souder, "Impurities and Trapping States in Calcium Tungstate", Phys. Lett., 24A, 246 (1967)

41. V. Schaefer, "Untersuchung der Lumineszenzabklingung von Wolframatleuchtstoften nach Anregung mit UV-Licht und Electronen", 2. Phys., 166, 429 (1962)

42. K. Reibner, A. Scharmann, "Photoleitfähigkeit von $CaWO_4$-Einkristallen", Z. Phys., 191, 480 (1966)

43. K. H. Nicholas, J. Woods, "The Evaluation of Electron Trapping Parameters from Conductivity Glow Curves in Cadmium Sulphide", Brit. J. Appl. Phys., 15, 783 (1964)

44. P. Braunlich, A. Scharmann, "Ein Einfaches Model fuer die Deutung der Thermolumineszenz und der Thermisch-stimulierten Leitfaehigkeit von Alkalihalogeniden", Z. Phys., 177, 320 (1964)

45. P. J. Kelly, M. J. Lanbitz, "On the Analysis of Glow Curves", Can. J. Phys., 45, 311 (1967)

46. J. T. Randall, M. H. F. Wilkins, "Phosphorescence and Electron Traps, I. Study of Trap Distribution", Proc. Roy. Soc., 184A, 366 (1945)

47. A. Wrzesinska, "Impurity Activated Crystalline Phosphors - Their Production and Thermoluminescence Curves", Acta Physica Polonica, 15, 151 (1956)

48. L. I. Grossweiner, "A Note on the Analysis of First-Order Glow Curves", J. Appl. Phys., 24, 1306 (1953)

49. J. Urbach, Cornell Symposium (1948)

50. M. L. Katz, Izd. Saratovsk gos. Univ. (1960)

51. L. M. Rabkin, D. S. Konevskaya, "Thermoluminescence and Capture Levels in $CaTiO_3$:Pr", Sov. Phys. Sol. State, 8, 794 (1966)

52. C. Bucci, R. Fieschi, G. Guidi, "Ionic Thermocurrents in Dielectrics", Phys. Rev., 148, 816 (1966)

53. P. Scaramelli, "F' and M' Traps in Alkali Halides Studied by Means of Photostimulated Thermoluminescence", II Nuovo Cimento, XLV, 119 (1966)

54. H. Gobrecht, D. Hofmann, "Spectroscopy of Traps by Fractional Glow Technique", J. Phys. Chem. Sol., 27, 509 (1966)

55. H. D. Vasileff, "Thermal Ionization of Impurities in Polar Crystals. I. Formal Theory", Phys. Rev., 96, 603 (1954)

56. H. D. Vasileff, "Thermal Ionization of Impurities in Polar Crystals. II. Application to Interstitials in Cubic ZnS", Phys. Rev., 97, 891 (1955)

57. H. A. Koehler, D. R. Mason, C. Kikuchi, "Trap Depth and Frequency Factor Determination from Thermoluminescence Peaks", Bull., Am. Phys., 12, 896 (1967)

58. D. R. Mason, H. A. Koehler, C. Kikuchi, "Identification of Defect Sites in $CaWO_4$ from the Correlation of ESR and Thermoluminescence Measurements", Phys. Rev. Lett., 20, 451 (1967)

59. D. R. Mason, H. A. Koehler, C. Kikuchi, S. Irizarry-Milan, "ESR Identification of $CaWO_4$ Thermoluminescence Centers by Differential Thermal Annealing", Bull, Am. Phys., 13, 436 (1968)

60. H. Zeldes, R. Livingston, "Paramagnetic Resonance Study of Irradiated Single Crystals of Calcium Tungstate", J. Chem. Phys., 34, 247 (1961)

61. C. E. Barnes, "Thermal-Neutron-Induced Defects in Cadmium Telluride and Cadmium Sulfide", Doctoral Thesis, Nuclear Engineering Department, University of Michigan (1967)

62. NBS Circular 539, 6, 23 (1956)

63. K. C. Chu, C. Kikuchi, "Direct Measurement of the Oxygen Vacancies Produced in Calcium Tungstate by Fast Reactor Neutrons", (to be published in Phys. Rev.)

64. C. F. Hempstead, K. D. Bowers, "Paramagnetic Resonance of Impurities in $CaWO_4$. I. Two S-State Ions", Phys. Rev., 118, 131 (1960)

65. P. Chester, "Cross-Doping Agents for Rutile Masers", J. Appl. Phys., 32, 866 (1961)

66. T. T. Chang, "Paramagnetic Resonance Spectrum of W^{+5} in Rutile (TiO_2)", Phys. Rev., 147, 264 (1966)

67. K. C. Chu, "Electron Spin Resonance of Paramagnetic Tungsten and Niobium Substitution in Calcium Tungstate", Doctoral Thesis, Nuclear Engineering Department, University of Michigan (1967)

68. "Gmelins Handbuch der Anorganischen Chemie: Wolfram", Vol. 54, Verlag Chemie, GMBH., Berlin, 1935, p:117

69. H. Azarbayejani, "ESR of W^{+5} in $CaWO_4$:Y", Bull., Am. Phys., 10, 1131 (1965)

70. W. G. Wyckoff, "Crystal Structure", Vol. 2, Interscience Publ., New York, 1963, p:82

71. A. Zalkin, D. H. Templeton, "X-Ray Diffraction Refinement of the $CaWO_4$ Structure", J. Chem. Phys., 40, 501 (1964)

72. Vinokurov, et al., "Paramagnetic Resonance of Nb^{+4} Ion in Zircon Single Crystals", Sov. Phys. Solid State, 5, 1487 (1964)

73. S. Karavelas, "Molecular Orbital Theory of Vanadium in the Rutile Structure Crystals SnO_2, TiO_2, GeO_2", Doctoral Thesis, Nuclear Engineering Department, University of Michigan (1964)